White Rose Research Online

eprints@whiterose.ac.uk
https://eprints.whiterose.ac.uk
Universities of Leeds, Sheffield and York

Deposited via The University of Leeds.

White Rose Research Online URL for this paper:
https://eprints.whiterose.ac.uk/id/eprint/182248/

Version: Accepted Version

Article:
Shi, Y-G, Jiang, L, Lin, S et al. (2022) Ultra-efficient antimicrobial photodynamic inactivation system based on blue light and octyl gallate for ablation of planktonic bacteria and biofilms of Pseudomonas fluorescens. Food Chemistry, 374. 131585. ISSN: 0308-8146

https://doi.org/10.1016/j.foodchem.2021.131585

© 2021 Elsevier Ltd. All rights reserved. This manuscript version is made available under the CC-BY-NC-ND 4.0 license http://creativecommons.org/licenses/by-nc-nd/4.0/.

Reuse
This article is distributed under the terms of the Creative Commons Attribution-NonCommercial-NoDerivs (CC BY-NC-ND) licence. This licence only allows you to download this work and share it with others as long as you credit the authors, but you can't change the article in any way or use it commercially. More information and the full terms of the licence here: https://creativecommons.org/licenses/

Takedown
If you consider content in White Rose Research Online to be in breach of UK law, please notify us by emailing eprints@whiterose.ac.uk including the URL of the record and the reason for the withdrawal request.

UNIVERSITY OF LEEDS
University of Sheffield
UNIVERSITY of York

Highlights:

- OG worked as an intriguing photosensitizer in aiding the photodynamic inactivation
- The PDI was efficient at eradicating planktonic *P. fluorescens* and its biofilm
- The mode of bactericidal action of OG-mediated PDI was systemically investigated
- Bacterial inactivation by PDI might be due to multi-damage to cellular components
- Nanofibers in combination with PDI have superiorities for salamander preservation

Manuscript Click here to view linked References

Submit online to *Food Chemistry*

Manuscript Number:

Title

Ultra-efficient photodynamic inactivation system based on blue light and alkyl gallate for synergistic antibacterial and ablation biofilms against *Pseudomonas fluorescens* and smart application with electrospun nanofibers on Chinese giant salamander preservation

Yu-gang Shi [a,b], Lai Jiang [a,b], Shan Lin [a,b], Wen-gang Jin [c], Qing Gu [a,b], Yue-wen Chen [a,b], Ke Zhang [a,b], Rammile Ettelaie [d]

[a] School of Food Science and Biotechnology, Zhejiang Gongshang University, Hangzhou, Zhejiang 310035, China
[b] Institute of Food Microbiology, Zhejiang Gongshang University, Hangzhou, Zhejiang 310035, China
[c] *Bio-resources Key Laboratory of Shaanxi Province, School of Biological Science and Engineering, Shaanxi University of Technology, Hanzhong 723001, China*
[d] *School of Food Science and Nutrition, University of Leeds, Leeds, LS2 9JT, UK*

Corresponding Author:

Yu-gang Shi
School of Food Science and Biotechnology, Zhejiang Gongshang University, Xiasha University Town, Xuezheng Str. 18, Hangzhou 310018, China
Tel.: 86-0571-28008927
E-mail: yugangshi@zjgsu.edu.cn

ABSTRACT

Pseudomonas fluorescens is a Gram-negative spoilage bacterium and dense biofilm producer, which will cause food spoilage and persistent contamination. Here, we report an ultra-efficient photodynamic inactivation (PDI) system based on blue light (BL) and a multifunctional food additive, octyl gallate (OG) to eradicate bacteria and biofilm of *P. fluorescens*. OG can rapidly penetrate the cells and produce a high-level toxic reactive oxygen species (ROS) triggered by BL irradiation. Both OG and ROS are critical to destroying the bacterial membranes and rupture cell bodies, causing protein components alterations and DNA fragmentation in bacteria. Moreover, OG plus BL irradiation can efficiently not only prevent the formation of biofilms but also scavenge the existing biofilms. Additionally, the situ photodynamic antibacterial activity of OG/PLA electrospun nanofibers was evaluated during the salamander storge. Our studies prove that the OG-mediated PDI can provide a simple and ultra-effective platform for combating bacteria and eradicating biofilm.

Keywords: Photodynamic inactivation; alkyl gallates; antimicrobial mechanism; reactive oxidative species; electrospun nanofibers; *Pseudomonas fluorescens*

1. Introduction

Pseudomonas fluorescence is a food spoilage bacterium largely responsible for the deterioration of aquatic products and dairy products, which can grow well at low temperatures and facilitate the spoilage of aquatic products in cold-chain transportation as compared with other spoilage (Caldera et al., 2016). Worse still, *P. fluorescence* cells can attach to food contact surfaces and form biofilms readily, making it more difficult to be eliminated. Meanwhile, the biofilm protects organisms against desiccation, biocides, some antibiotics and metallic cations, ultraviolet radiation (Flemming & Wingender, 2010). To avoid these problems, antibiotics are often used to reduce their threat, but indiscriminate use of antibiotics often might facilitate the emergence of drug resistance. Therefore, it is urgent to develop efficient strategies to kill *P. fluorescence* and eradicate its biofilm.

As distinguished from traditional thermal-based technologies used for foods decontamination, some non-thermal procedures including ultrasound, cold plasma, high hydrostatic pressure, pulsed electric field, and pulsed light processing have been developed to inhibit the growth of microorganisms and preserve nutritional quality and sensory acceptability of food (Ortega-Rivas & Salmerón-Ochoa, 2014). Despite such significant potentials, some limitations, such as low compatibility for broader food applications, higher processing requirements and costs, as well as the emergence of microbial tolerance, limit the wide application of them (Cebrian et al., 2016). Recently, a novel emerging non-thermal processing by light called photodynamic inactivation (PDI) is gaining focus and are being applied for microbial growth control in the food industry (Ferrario et al., 2015). PDI is an athermal photochemical reaction based on the combination of the simultaneous presence of light, and photosensitizers (PSs) and oxygen (Luksienė & Zukauskas, 2009). Bacteria containing PSs have the ability to absorb light at specific wavelengths. Once the light is absorbed, the PS gets excited to a higher energy state under the presence of oxygen. On their way back to the ground state, they collide with oxygen in the cytoplasm, transferring energy and subsequent producing high reactive oxygen species (ROS). The ROS would interact with adjacent intracellular components, such as lipids, proteins and nucleic acids, leading to bacterial death (Nakamura et al., 2012). Although UV light has been widely used to decontaminate foods and inactivate various foodborne pathogens and biofilm cells, it has restricted application in the food industry due to its low penetration ability for solids or opaque liquids and causing serious eye and skin damage to food operators, as well as food sensory degradation (Kim et al., 2016). In contrast, LEDs can also effectively inactivate pathogens and preserve food in postharvest stages and avoid the mentioned issues related to UV radiation (D'Souza Yuk, Khoo, & Zhou, 2015). LED technology being low-hazard (no mercury), low energy consumption, safe and high durability, as well as broader and

higher antibacterial effect on microorganisms, LED-based PDI have recently been explored more and more as a novel preservation technology in food processing (Kim et al., 2017; Luksienė & Zukauskas, 2009).

Lots of studies in PDI focus on the synthesis or discovery of more effective PSs. They can be divided into endogenous and exogenous PSs from the source. Porphyrins are the most well-known natural endogenous PSs which are found in many bacterial and fungal cells (Rapacka-Zdonczyk et al., 2019). When the magnitude of inactivation with endogenous PSs is lower than desired, it is essential to use an exogenous PS to enhance it. At present, many artificially synthesized exogenous PSs, such as chlorine, phthalocyanines and phenothiazinium dyes, etc, show good photoactivity. However, safety considerations, organoleptic changes and consumer perceptions associated with the use of an exogenous PS are also crucial to the application of PDI in food processing. Thus, natural exogenous PSs such as hypericin, Vitamin K3 (Sheng et al., 2020), and curcumin are good candidates for food application, given that they have no toxic or genotoxic effects. Recently, phenolic compounds, especially phenolic acids, have been extensively studied in the food industry due to their various bioactive properties, especially antimicrobial activities. Limited studies have directly utilized them including gallic acid (GA), caffeic acid (CA), chlorogenic acid as PSs to generate ROS including H_2O_2 and •OH radicals under the exposure of blue light in the presence of dissolved oxygen, effectively inactivating bacteria (Nakamura et al., 2012; 2015; 2017). Electrons are transferred from photo-oxidized polyphenols to dissolved oxygen to produce H_2O_2, which is then photolyzed by blue light to produce •OH radicals (Nakamura et al., 2013), as the main contributor to the bactericidal activity of such PDI. Besides, PDI technology based on photo-oxidation of CA has been developed to eliminate *S. mutans* biofilm (Nakamura et al., 2017). On the other hand, our research group has long been engaged in the study of the antibacterial activities and mechanism of a variety of phenolic acids and their ester derivatives (Shi et al., 2018; 2020; 2021). Some of them have been found to exhibit stronger antibacterial and anti-biofilm activities against foodborne pathogens, compared to the corresponding phenolic acids. Among them, octyl gallate (OG) showed the superior interaction/affinity with membranes and antibacterial activity against *E. coli* and *S. aureus* (Shi et al., 2020), as well as *P. fluorescence* (Zhang et al., 2021). Surprisingly, the potential of OG with low concentration as a novel PS for PDI has been found in this work, which endows OG-mediated PDI with intriguing bactericidal efficacy to achieve rapid eradication of pathogens and biofilms in a relatively short time due to both photodynamic and intrinsic antibacterial properties of OG itself. Besides, since OG has been permitted for use as an antioxidant additive in food (FDA, 2001a, 2001b), it is supposed to be safe for humans and can be

considered as an alternative exogenous PS of PDI. Additionally, electrospinning is one of the promising encapsulation methods in which a variety of active substances are encapsulated in the nanofiber matrix (Wen et al., 2017). Electrospun nanofibers with a large surface area to mass ratio have been proposed for stabilizing or controlling the release of the active compounds such as antibacterial agents in food processing and packaging (Kayaci & Uyar, 2012), showing longer lasting antibacterial activity. Recently, we successfully utilized OG as a multi-functionalized food additive combined with the advantages of electrospinning nanofibers for the preservation of Taihu icefish in China (Shi et al., 2021). Therefore, inspired by the combination of these ideas, we chose OG as a photosensitizer combined with blue light to inactivate *P. fluorescence*, and further developed an ideal antibacterial strategy based on the combination of PDI and electrospinning nanofibers to protect sea foods from spoilage bacteria, avoid their quality degradation and flavor loss and extend the shelf life during storage.

Herein, the aim of the present study was to examine the synergistic effect of octyl gallate (OG) and blue light (BL) to inhibit the growth of *P. fluorescence* planktonic bacteria as well as eradicate its biofilm, and further elucidate the mode of action. Besides, we investigated electrospun nanofibers embedded with the photosensitizer OG as a PDI-based packaging material and evaluated its antibacterial activity in the storage and preservation of Chinese giant salamander. The dual role of OG in improving the production of ROS as a novel PS on one hand and the enhanced antimicrobial activity as an effective antibacterial on the other, are highlighted for the first time.

2. Materials and methods

2.1. Materials and light source

Octyl gallate (OG) was prepared by us and the structure was characterized by ^{1}H NMR and ^{13}C NMR. *β*-cyclodextrin (*β*CD) was purchased from Aladdin and acetic acid (99%, analytical reagent grade) was obtained from Macklin, Shanghai. All other reagents used were of analytical grade. Light-emitting diode arrays (420 nm, 10×10 cm, 90 W×2; Xuzhou Aijia Electronic Technology Co., Ltd, China) with an emission maximum of 420 nm as a light source were used for PDI. The blue LEDs were enclosed by deep photo accessories to avoid the entry of light from outside and the LED system was equipped with a cooling fan and a heat sink to dissipate the heat. For irradiation, the light sources were placed at 1.0 cm from the samples. The illumination energy of blue LED (212 mW/cm^2) was determined by using an energy meter console (PM100D, Thorlabs, New Jersey, USA) attached with a photodiode power sensor (S120VC, THORLABS, Newton, USA). The dosage (in J/cm^2) received by each bacterial suspension was calculated by multiplying the intensity (in W/cm^2) by the irradiation time (in seconds).

2.2. Microorganisms

P. fluorescens isolated from Russian sturgeon (*Acipenser gueldenstaedti*) by us (Zhang et al., 2021) and *S. aureus* ATCC 6538 (CMCC, Beijing, China) were used in this study. The pre-cultured bacterial cells were inoculated into the fresh Luria-Bertani (LB) medium (Hangzhou Microbial Reagent, Co. Ltd, China), and grown to an exponential phase at 30 °C and 37 °C, respectively, with the agitation of 180 rpm. They were used as indicator strains for all experiments to evaluate the inhibitory activity of OG-mediated PDI.

2.3. Antimicrobial activity of PDI on the planktonic P. fluorescens in vitro

The OG+BL treatments were performed according to the methods (Nakumura et al., 2012) described before. The overnight bacterial culture of *P. fluorescens* was diluted in sterilized 0.1, 0.2 and 0.4 mM OG (or GA) solution prepared in normal saline to reach a final concentration of approximately 6 Log CFU/mL. Then, 5 mL of the bacterial suspension was transferred to a glass tube and followed immediately by BL exposure applied for 0 ~ 30 min (Irradiation intensity: 212 mW/cm^2, distance:1 cm). Bacterial suspension incubated in the dark with OG (or GA) for the same

duration was used as a control. Next, the treated solution was serially diluted in 0.9% (w/v) saline, after which 100 µL of the dilution was seeded on LB agar plates. The plates were incubated at 30 °C for 24 h before enumeration, and the reductions of bacteria were determined. To confirm whether the bactericidal effect of PDI might be associated with ROS, ROS scavengers CAT (1200 U/mL), DMSO (2.8 M) and TEMPOL (16 mM) were added simultaneously with OG. The cultured bacterial with ~6 Log CFU/mL *P. fluorescens* was treated in the absence or presence of BL light for 15 min. The control without ROS inhibitor was incubated in the dark for the same duration. Subsequently, the standard plate counting method described in 2.3. was performed on all samples.

2.4. Mechanism studies of the synergistic antibacterial treatment

2.4.1. Association of OG or GA with P. fluorescens

The uptake of OG (or GA) in *P. fluorescens* cells with or without BL irradiation was measured by using diphenylboric acid 2-aminoethyl ester (DPBA) (Shi et al., 2021). A volume of 1 mL 0.9% (w/v) saline containing 8 Log CFU/mL *P. fluorescens* was mixed with or without GA or OG (0.4 mM). Then, 1 mL of the bacterial suspension was added to a 24-well plate (Costar 3599, Corning, USA) and exposed to BL for 20 min as described previously. Controls were treated in the same manner, but in the absence of phenolics or BL irradiation. Then, each sample was transferred back to the tube and centrifuged at 10,000×g for 5 min to remove the supernatant. The pellet was washed twice using DI water followed by vortexing and then DPBA solution (450 µL, 0.2%, w/v, in DMSO) was added to the pellet and then incubated for 5 min. The final suspension (200 µL) was transferred to a 96-well plate and the fluorescence intensity was measured at excitation/emission wavelength of 405/465 nm using a microplate reader (Synergy H1, BioTek, Winooski, VT, USA). The fluorescence intensity (I) ratio was corrected using the following equation:

$$I_{corrected} = I_{sample} - I_{control}$$

where I_{sample} stands for the fluorescence intensity of the sample exposed to the treatment and $I_{control}$ stands for the fluorescence intensity of the control.

Quantification of phenolics (OG or GA) adsorption was also observed through confocal laser scanning microscopy according to the method reported by Wang et al. (2017) with some modifications. Detailed descriptions are given in SI (Section 1.1)

2.4.2. Analysis of reactive oxygen species (ROS)

2',7'-dichlorofluorescein diacetate (DCFH-DA) was used to assess the generation of ROS in the bacterial cells (Shi et al., 2021). The overnight test culture (8 Log CFU/mL) was treated by OG (0.4 mM) with or without ROS scavengers including catalase (CAT), dimethyl sulfoxide (DMSO) or TEMPOL. The CAT, DMSO or TEMPOL solution was added into a sample solution to achieve a final concentration of 1200 U/mL, 2.8 M and 4 mM, respectively. The suspensions were incubated in the dark with OG for the same duration were used as positive controls. After BL irradiation for 20 min, the excess OG in samples was removed by centrifugation (10000×g, 4 °C, 5 min) and the bacteria were resuspended with cold phosphate-buffered saline (0.1 mM PBS, pH 7.2-7.4). 10 μM DCFH-DA was mixed with samples and treated in dark at 30 °C for 30 min. The incubated solution was washed twice using PBS to remove excess dye. Finally, the fluorescence spectrum of solutions was measured at excitation wavelengths of 485 nm with a wavelength of 525 nm with a microplate reader (Synergy H1 Multi-Mode Reader, BioTek, Winooski, VT, USA). Bacterial suspension with water treated in the dark was considered as a negative control, and its fluorescence intensity (F_o) was used as the reference to calculate the relative fluorescence unit (RFU) for other treatments using the equation:

$$\text{Relative fluorescence unit (RFU)} = F_s/F_0$$

where F_s was the fluorescence intensity of the sample with treatments.

Finally, to visualize the ROS generated by PDI treatment, the confocal laser scanning microscope (CLSM, Leica TCS SP8, Germany) using ×63 oil immersion objective lens was used to observe the cells at excitation/emission wavelength of 484/525 nm.

2.4.3. Hydroxyl radical experiments using flow cytometry.

Flow cytometry was used to detect hydroxyl radical formation. Hydroxyphenyl-fluorescein (HPF) is an anthracene derivative of fluorescein which becomes fluorescent when it was activated by hydroxyl radical (Shi et al., 2021). Detailed descriptions of the method are given in SI (Section 1.2).

2.4.4. Investigation of the cell membrane damage

To evaluate the cell membrane damage induced by OG+BL treatment, the uptake of propidium iodide (PI) and scanning electron microscope (SEM) were performed according to our previously

published papers (Shi et al., 2020; 2021). Detailed descriptions of the methods are given in SI (Section 1.3).

2.4.5. Sodium dodecyl sulfate-polyacrylamide gel electrophoresis (SDS-PAGE)

SDS-PAGE analysis was performed to determine the alternations of bacterial proteins before and after the treatment of OG and BL irradiation. Detailed descriptions of the method are given in SI (Section 1.4).

2.4.6. Genome integrity determination

The damage of DNA caused by OG+BL was investigated by the agarose gel electrophoresis. Detailed procedures were offered in SI (Section 1.5).

2.5. Inhibition assay for biofilm formation

The assay method of Damiano et al. (2017) was carried out in 24-well flat-bottom polystyrene plates (Costar 3599, Corning, USA). Briefly, 100 μL of *P. fluorescens* (~7 Log CFU/mL) were diluted 1:10 into 900 μL of LB broth (1.0% tryptone, 0.5% yeast extract, 1.0% NaCl) in 24-well plates to obtain the final concentration of ~6 Log CFU/mL and then cultivated with for 0~96 h without agitation. After incubation, bacterial suspension of each well was gently decanted, the wells were washed 3 times with sterile PBS (0.1 M, pH 7.2) to remove planktonic bacteria and biofilms were stained for 30 min using crystal violet (0.1%, w/v). The stained biofilms were rinsed 3 times with distilled water and extracted with 1 mL of 95% ethanol. Biofilms were quantified at 600 nm by reading the microplates (Synergy H1 Multi-Mode Reader, BioTek, Winooski, VT, USA).

For determination of the effect of different treatments on biofilm formation, 100 μL of *P. fluorescens* (the original suspension was diluted to ~8 Log CFU/mL) were diluted into 900 μL of LB 24-well flat-bottom polystyrene plates containing (0.15 mM or 0.1 mM) OG (below the minimum inhibitory concentration), with ethanol serving as the control. After cultivation at 30 ^{o}C for 15 min in the absence or presence of BL irradiation (94.8 mW/cm^2, distance: 2 cm) (subinhibitory external condition). Biofilms were quantified by the crystal violet assay above.

To count planktonic bacteria, the suspension cultures (100 μL) were centrifuged at 5000 rpm at 4 °C to collect the pellets, which were resuspended in 1 mL of 0.9% NaCl and 10-fold serially diluted for enumeration.

2.6. Per-formed biofilm eradication assay

P. fluorescens biofilms were incubated as described above. In brief, 100 μL of *P. fluorescens* were added to 900 μL of LB to obtain the final concentration of ~6 Log CFU/mL (as described before) and then cultivated at 30 ºC for 60 h without agitation. The bacterial suspension was discarded and wells were rinsed 3 times with sterile PBS to remove the loosely attached bacteria. To evaluate the effect of OG on the biofilm, OG concentrations in fresh LB medium were added to the pre-formed biofilm in the wells, with ethanol serving as an extra negative control. The plates were cultivated at 30 °C for 30, 60 and 90 min without shaking in the absence or presence of BL irradiation (212 mW/cm^2). Biofilms were fixed with methanol for 15 min and staining was performed as before. To quantify cell viability in biofilm, the treated biofilms were washed with PBS three times and swabbed using a sterile cotton swab (Nakumura et al., 2017). The collected bacteria were suspended in 1 mL of saline, and the mixture was serially diluted 10-fold with saline, and 100 μL of the dilution was plated on LB agar at 30 °C overnight. On the other hand, for viable colony counts of planktonic cells, the suspension cultures after treatments were diluted 10-fold with saline, and the dilution (100 μL) was plated on LB agar for enumeration of planktonic cells.

2.7. Confocal laser scanning microscopy (CLSM)

To observe the formation of the biofilm after various treatments, samples were captured by CLSM refer to Seo and Kang (2020) with some modifications. Biofilm was stained using a LIVE/DEAD *Bac*light Bacterial Viability Kits (Molecular Probes, Invitrogen, USA) according to the manufacturer's instructions. The biofilm was washed with PBS and visualized using a CLSM. More details were given in SI (Section 1.6).

2.8. Preparation of nanofibers (NFs)

The NFs were prepared using the method reported by us (Shi et al., 2020) with some modifications. More detailed descriptions of the method are given in SI (Section 1.7). The morphology of The collected fibers was observed via SEM (Hitachi T-1000, Hitachi High-Technologies Corporation,

Tokyo, Japan) (see Fig. S1) and the preservation of giant salamander was shown in Fig. S4.

2.9. In situ antibacterial activity of OG/PLA NFs

To assess the synergistic effect of OG/PLA NFs and PDI on the preservation of Chinese giant salamander, the changes in the total viable count and flavor of samples during storage were studied. The salamander meat cubes were inoculated by immersion in a bacterial suspension of *P. fluorescens* (3 Log CFU/mL) for 30 seconds. The treated salamander meats were singly sealed with OG/PLA NFs and followed immediately by BL exposure for 30 min at a distance of 1 cm. Meanwhile, to evaluate the quality of the giant salamander with different treatments during the storage, the electronic nose was applied. More details were given in SI (Section 1.8 and 1.9).

2.10. Statistical analysis

Results were expressed as mean ± standard deviation. T Statistical significance between different treatments was determined using t-test; *P*-values ≤ 0.05 were used to determine significant differences.

3. Results and discussion

3.1. Bactericidal effect of the OG-mediated PDI on P. fluorescens cells suspension

We evaluated the use of BL illumination in combination with OG as an alternative approach to achieve *P. fluorescens* inactivation (Fig. 1). *P. fluorescens* was killed synergistically by BL combined with OG in both BL and OG dose-dependent manners in planktonic solutions. As shown in Fig. 1A-(a), viable bacterial counts for *P. fluorescens* without any treatment were ~6.5 Log CFU/mL, while a significant reduction was observed in the sample treated by BL irradiance (190.8 J/cm^2) for 15 min. OG inhibited the growth of *P. fluorescens* in an OG concentration-dependent manner, and the OG-mediated PDI led to higher antibacterial potency as compared with those equivalents in the absence of BL irradiation ($P<0.01$). Under 190.8 J/cm^2 irradiation of BL, the *P. fluorescens* cells were decreased from 3.8 to 1.8 Log CFU/mL when the OG concentration was elevated from 0.1 to 0.2 mM. Moreover, bacterial cells could not be detectable from the samples treated by BL irradiation with 0.4 mM OG. In Fig. 1A-(b), compared to the positive controls with only BL irradiation, significant decreases of bacterial cells were observed in samples with the

OG-mediated PDI (P<0.01). Also, the BL irradiation time (dosage) significantly influenced the activity of *P. fluorescens.* After 10 min irradiation with OG (0.1, 0.2 and 0.4 mM), the cells were decreased to 4.5, 3.5 and 2.2 Log CFU/mL (P<0.05), respectively. However, an obvious and continuous decrease in the bacterial cells was achieved when PDI irradiation time was extended from 10 to 15 min. Thus, these findings ensure that the efficacy of OG-mediated PDI-induced inactivation against *P. fluorescens* was typically dependent on the photosensitizer concentration and irradiation dosage.

In Fig. 1B, when the Gram-negative *P. fluorescens* and Gram-positive *S. aureus* were treated with the OG-mediated PDI, viable counts decreased in a time-dependent manner. Moreover, *S. aureus* tended to show higher susceptibility to the OG+BL treatment than *P. fluorescens*. It may be due to that the *S. aureus* was more susceptible to OG than *P. fluorescens*. Also, the MIC and MBC values of OG against *S. aureus* are lower than those against *P. fluorescens* (Table S1). Although treatment with OG or BL irradiation performed in this present study could cause a reduction in the remaining bacterial count, BL irradiation of the suspension containing 0.4 mM OG could significantly kill the bacteria within 15 min. A stronger synergistic effect on bacteria in vitro was found when OG was combined with BL illumination.

Cossu et al. (2016) also reported that a synergistic interaction between 10 mM gallic acid (GA) and UV-A (365 nm) light could inactivate *E. coli* O157:H7. Nakamura et al. (2012) reported that >5-Log CFU/mL reduction was obtained when the suspension of *S. aureus* was co-incubated with 4 mM gallic acid (GA) for 15 min when exposed to LED light (400 nm; 80 mW/cm^2). By contrast, in the present study, neither GA alone nor the combined treatment with BL irradiation showed a substantial bactericidal effect (<1-Log). Moreover, under the dark condition, OG showed higher bactericidal activity than GA (Fig. 1B). Also, it should be noted that although GA has antimicrobial activity, OG exerted stronger inhibitory capacity than GA because Gram-negative *P. fluorescens* and Gram-positive *S. aureus* were effectively killed by OG in LB media, at very low concentration, presenting an MBC of 3.2 mM for *P. fluorescens* and 0.1 mM for *S. aureus* (Table S1), respectively. Wang et al. (2017) reported that the effect of propyl gallate (10 mM)+UV-A on the inactivation of *E. coli* O157:H7 was stronger than that treated by GA (10 mM)+UV-A. These findings suggest that (1) the antimicrobial potency of OG depends largely on the hydrophobic portion (the alkyl group) of the molecule, which is also in agreement with the findings reported by Kubo et al. (2004) and us (2021). (2) As for the OG-mediated PDI, OG alone or BL irradiation does not solely contribute to the remarkable reduction in the CFU of bacteria, reliably suggesting the

occurrence of interaction between OG and BL.

[Fig. 1.]

3.2. Antimicrobial mechanism of the OG-mediated PDI against P. fluorescens

3.2.1. Interaction between OG and bacterial cells

The remarkable photosensitizing efficiency of OG suggests that it could be exploited to obtain efficient bacterial photoinactivation. To gain further insight into the mechanisms underlying the antibacterial effects of OG-mediated PDI, we firstly analyzed the binding affinity of OG toward bacteria. In the present case, DPBA has been employed to detect the cellular uptake of OG or GA in *P. fluorescens*. It is a specific dye that becomes fluorescent when it was combined with flavonoid compounds (Shi et al., 2021). Fig. 2A shows that *P. fluorescens* treated with OG+BL has a higher fluorescent intensity (3179±294.0) than that incubated with OG alone (1147±41.9), indicating that the BL irradiation increased the level of OG uptake in *P. fluorescens*. Also, the extent of uptake of OG is significantly stronger (P<0.05) than that of GA regardless of the absence or presence of BL irradiation, indicating that OG shows higher binding affinity capacity to bacteria compared to GA. Moreover, the either OG or GA uptake results happen to coincide with their inactivation results in Fig. 1B, indicating that the cellular uptake of OG was a vital element for OG-mediated PDI and the higher uptake of OG under BL irradiation enhanced the antimicrobial effect. Their discrepancy in the affinity to bacteria could be explained by their different hydrophobicity. The Log P value of OG is 4.63 while it is 0.4 for GA (Table S1). Both of them possess the same hydrophilic portion, the pyrogallol group, thus distinguishing the role of the hydrophobic alkyl portion of OG, as discussed in our previous studies (Shi et al., 2018, 2019, 2021). The enhanced association of OG toward bacteria was further determined by using confocal microscopy. In Fig. S2, the amount of OG internalized by or bound tightly with bacterial cells was remarkably more than that of GA during the same period, further corroborating that the affinity to bacteria varied with the alkyl chain length. Compared to GA, amphiphilic OG could more effectively bind to bacteria, leading to increased intracellular uptake. These results illustrated that OG as an alternative antimicrobial photosensitizing agent induced a more effective photokilling of pathogenic microbial cells than GA.

3.2.2. OG and BL induced ROS generation

It had been reported that ROS generation, especially interior hydroxyl radicals (•OH), is a critical

step for the bactericidal effect of BL irradiated polyphenols (caffeic acid, chlorogenic acid, gallic acid, and proanthocyanidin) against a broad range of pathogens in the presence of dissolved oxygen (Nakamura et al., 2015). Moreover, the reaction began with the photo-oxidation of the polyphenolic hydroxyl group. As such, upon reaching the cells and following light activation, it is reasonable to speculate that OG may be also excited by BL to generate ROS. Thus, to evaluate the generation of ROS in *P. fluorescens* induced by photoirradiated OG, DCFH-DA was used as a fluorescent probe as it can be oxidized by cytosolic ROS to green fluorescent 2',7'-dichlorofluorescein (DCF). As shown in Fig. 2B, bacteria treated by the BL irritation had significantly higher fluorescent intensity than the corresponding samples without BL irradiation. Moreover, cells treated by OG+BL showed the strongest fluorescent intensity, followed by bacteria treated with OG alone in the dark, representing the efficient intracellular ROS production during the combination OG with the exposure of BL. Even though *P. fluorescens* treated by GA had significantly lower fluorescent intensity than bacteria treated by OG regardless of BL irradiation, GA with BL irradiation for 30 min could cause a higher fluorescent intensity as compared to samples treated by GA in dark. It is noteworthy that these findings are also in consistency with their antibacterial capacities in Fig. 1B. It indicated that ROS production plays a crucial role in OG-mediated photokilling and OG is a superior photosensitizer as compared to GA. To further visualize the generation of ROS induced by OG+BL treatment, *P. fluorescens* cells exposed to the selected treatments were observed using a confocal laser scanning microscope (CLSM). In Fig. 2C, the combination of OG with BL irradiation caused a higher level of ROS than both controls and OG alone, indicating that BL irradiation played an important role in the production of ROS. To further ascertain the specific ROS generation in OG-mediated PDI, the bacteria were incubated in the presence of several radical scavengers. We exposed OG-treated *P. fluorescens* to the H_2O_2 scavenger (CAT), •OH scavenger (DMSO), and $•O_2^-$ scavenger (TEMPOL), respectively, in the absence or presence of BL irradiation. In Fig. 2D-(a), the addition of these scavengers could significantly reduce the relative fluorescence unit as compared to the positive controls treated with OG alone. Moreover, as for BL irradiated samples, CAT and DMSO led to a higher level decline in the relative fluorescence unit than TEMPOL. Besides, the importance of intracellular ROS formation in the bactericidal activity of the duo was established by the ability of either CAT or DMSO (Fig. 2D-(b)). These findings indicated that the OG and BL interaction promoted the production of ROS (mainly, H_2O_2 and •OH) which is essential for OG-mediated PDI. Additionally, the intracellular •OH formation in the bactericidal action of OG-mediated PDI was also confirmed by the flow cytometry with the dye HPF, which was specifically oxidized by •OH radicals. The histogram distribution in Fig. 2E showed the contents of intracellular •OH radicals of different groups. Compare to the samples exposed to OG or BL alone,

a higher hydroxyl radical content was observed in bacteria treated with OG+BL. Moreover, we found DMSO significantly reduced the level of •OH induced by the duo. Together, these results imply that •OH radicals formation in *P. fluorescens* is directly related to OG-mediated PDI.

Akagawa et al.(2003) reported that catechins and other polyphenolic compounds could induce H_2O_2 generation in solutions under neutral or alkaline conditions. Also, it was found that H_2O_2 synthesis by (−)-epicatechin gallate is attributed to its bactericidal activity, which increases at higher pH values (Arakawa, Maeda, Okubo, & Shimamura, 2004) and a possible mechanism for H_2O_2 generation in a catechin solution was proposed by Mochizuki et al. (2002). In this case, blue light might trigger H_2O_2 photolysis to form •OH, further bolstering the bactericidal activity of the duo because •OH is the most destructive of all ROS to bacteria (Nakamura et al., 2015). And it has been reported that 500 mM H_2O_2 can kill *S. aurous* only with 1-Log reduction (Kanno et al., 2012). Thus, it is reasonable to assume that H_2O_2 would probably act as a source of •OH in the photolysis reaction, rather than be a major contributor to the bactericidal action in a short time (15-30 min), which is in agreement with the results reported by Nakumura et al. (2012). On the other hand, it has been proved that the internalized OG may interfere with the activity of ETC on the cytoplasmic membrane to produce toxic •OH, further leading to cellular damage and death (Shi et al., 2021; Kubo et al., 2004). Therefore, we inferred that the ROS observed in the present study may be produced directly by OG upon oxidation by BL in bacteria, and by indirectly mediating ROS formation through activating a variety of intracellular metabolic pathways. A possible scheme for potential pathways linking intracellular ROS generation induced by OG-mediated PDI is illustrated in scheme 1. The internalized OG may interfere with the activity of ETC on the cytoplasmic membrane, generating toxic ROS (Shi et al., 2021). More importantly, OG can be oxidized to quinone or hydroxyl related derivatives with the production of H_2O_2 using BL as the oxidizing source and oxygen as an oxidation catalyst, owing to the tendency of the three aromatic hydroxyl groups of OG to undergo autooxidation or oxidation (Wang et al., 2019). Then, H_2O_2 would be turned into •OH through the photolysis reaction by BL (Nakamura et al., 2015).

3.2.3. OG and BL induced alterations in the bacterial cell membrane, proteins and DNA

OG with a high affinity to the cell membrane may permeate the outer membrane to induce oxidative stress in bacterial cells. Then, the •OH generated around the phospholipid membrane will further have an effect on the structure and function of membranes. Some phenolic compounds had been observed to disintegrate the bacterial outer membrane (Shi et al., 2018, 2019). Thus, the membrane

damage of *P. fluorescens* was evaluated using PI as a fluorescent staining probe, and the increasing fluorescence signal represented the severe damage to the cytoplasmic membrane of cells (Stiefel, Schmidt-Emrich, Maniura-Weber, & Ren, 2015). In Fig. 2F, the presence of BL irradiation caused a significant increase ($P<0.05$) in the fluorescence intensity for all the treatments, compared to the corresponding samples in the dark. Although the fluorescence intensity of cells exposed to 0.4 mM GA+BL or BL irradiation alone (NS) was significantly higher than their correspondings, no bactericidal effect could be observed and logarithmic reduction of CFU/mL in these cases was <1-Log (Fig. 1B). Bacteria treated by OG+BL showed the strongest fluorescence intensity of PI, followed by the samples incubated with OG in the dark. However, only OG+BL treatment caused substantial inactivation (>5-Log) in the reduction of *P. fluorescens* within 15 min and *S. aureus* within only 10 min (Fig. 1B). It is interesting to note that the tendency in PI uptake happened to coincide with the findings of cellular uptake of phenolics in Fig. 2A, indicating cellular uptake of phenolics correlated positively with the damage of the bacterial membrane. SEM was used to further observe alternations in the surface morphology of bacteria treated by OG+BL. Samples treated by 0.4 mM OG without BL irradiation exhibit uneven and shriveled appearance (Fig. 2G-(b)), with a comparison of regular rod shape of controls (Fig. 2G-(a)). Serious damage to the cell walls of *P. fluorescens* occurred during the treatment of OG+BL with cell collapsing and the leakage of large cytoplasmic components (Fig. 2G-(c)), indicating that membrane damage was strongly associated with the bactericidal effect of OG+BL treatment.

The mentioned ROS may induce oxidative damage to the lipids, proteins and DNA of cells and ultimately led to bacterial death (Park et al., 2009). The alterations of membrane proteins of *P. fluorescens* upon OG-mediated PDI treatment were evaluated by using SDS-PAGE. Fig. 2H showed the similar band number and intensity of proteins from *P. fluorescens* without (Lane 1) or with BL irradiation (Land 2), implying that such dosage of BL irradiation had no effect on the membrane proteins integrity of *P. fluorescens*. OG at 0.4 mM only caused a slight decrease in the intensity of protein bands (Lane 3). In contrast, a significant decrease of band intensity (especially, for ~63 kDa and ~45 kDa protein) was observed from the sample treated with OG+BL irradiation and a new band (~35 kDa) was formed (Lane 4), highly suggesting that the OG-mediated PDI induced the great damage of membrane proteins and the exogenous photosensitizer (OG) might play a dominant role in eradicating *P. fluorescens*. DNA is the basis of normal physiological activities and the reproduction of bacteria. Except for the damage to the cell membrane and protein, the effect of OG-mediated PDI on the damage of genomic DNA of *P. fluorescens* is measured and shown in Fig. 2I. No significant changes in the band intensity of genomic DNA were observed in the sample

treated by BL irradiation alone compared to the control, indicating individual BL irradiation didn't display sufficient damage towards the genomic DNA of *P. fluorescens*. The band intensity of the group treated with OG or OG+BL was significantly decreased and the treatment of OG+BL almost completely wreck the integrity of genomic DNA of *P. fluorescens*, which is also consistent with both the generation of ROS in Fig. 2B and the antibacterial results in Fig. 1. These discrepancies of damage towards the genomic DNA could be reasonably explained by the difference in the generation of intracellular ROS induced by OG alone and OG+BL. These results are also consistent with the previous study of curcumin-mediated PDI on the genomic DNA of *L. monocytogenes* (Huang et al., 2020).

[Fig. 2.]

3.3. Proposed mechanism of OG-mediated PDI

A scheme of possible bactericidal action mechanisms of OG-mediated PDI is illustrated in Scheme 1. OG can interact with the bacteria cell membrane due to its high affinity to the membrane in terms of its hydrophobic portion to exert itself an excellent antimicrobial ability. Then, OG can induce membrane rupture and the leakage of cellular constituent materials, leading to the death of *P. fluorescens* (I). The internalized OG can further interfere with the activity of the electron transport chain (ETC) on the cytoplasmic membrane, causing increased production of toxic ROS including •OH (II) (Shi et al., 2021). On the other hand, the polyphenolic hydroxyl group of OG would be photo-oxidized by BL. Regarding oxidation, H_2O_2 could be produced through electron transfer from photo-oxidized OG to dissolved oxygen. The H_2O_2 is subsequently photolyzed by BL to generate •OH (III). Consequently, •OH from these two possible pathways would cause lethal oxidative damage to lipid, protein and DNA peroxidation, which further contribute to cellular damage and death. Moreover, OG-mediated PDI can interact simultaneously with multiple targets in the bacterial cells, like the cell membranes, lipids, proteins and DNA, making it difficult for bacteria to the development of antimicrobial resistance (Almeida, Faustino, & Tome, 2015). Thus, the combination of OG and BL irradiation could be considered a low-risk treatment for the development of bacterial resistance or tolerance due to their multitargeted modes of action.

[Scheme 1.]

3.4. Inhibitory effect of OG-mediated PDI on *P. fluorescens* of biofilm formation

P. fluorescens is high prevalence in the fish-processing industry and causes a serious problem due to adhesion to surfaces and biofilm mode of survival under severe conditions (Nilsson, Ross, & Bowman, 2011). Inspired by the highly bactericidal efficient and synergistic effect of OG+BL irradiation, the OG-mediated PDI was also expected to effectively inhibit biofilm formation of *P. fluorescens*. Before the PDI treatment, the biofilm formation of the *P. fluoresens* at 30 °C was determined by the crystal violet staining assay, and the results showed that 60 h was the optimal incubation time for the formation of *P. fluoresens* biofilm (Fig. S3). The inhibitory effect of OG+BL irradiation on *P. fluorescens* biofilm formation was presented in Fig. 3. The experiments in which planktonic *P. fluorescens* were first treated either with (0.05 and 0.1 mM) OG or BL irradiation (94.8 mW/cm^2) only, as well as OG+BL for 15 min and then left for 60 h to allow the recovery to form a biofilm, verified that the efficacy of OG+BL irradiation for the inhibition of biofilm formation. In Fig. 3A, when used alone, OG (0.05 mM) or BL irradiation treatment could not cause a significant reduction in the viability of planktonic cells compared to that of the negative control. Cell survival determination indicated that 0.05 mM OG coupled with BL irradiation had a slight effect on the viability of planktonic cells, though, at 0.1 mM, planktonic cells were reduced by only 12%. These results indicated that all treatments are performed under sub-lethal conditions have no or minor effect on the activity of *P. fluorescens*. In Fig. 3B, when samples were treated with BL irradiation alone, no significant change in biofilm formation was observed. Moreover, treatment with OG alone at 0.05 and 0.1 mM could induce a significant reduction in the formation of biofilms by 25% and 57%, respectively. Furthermore, at concentrations of 0.05 and 0.1 mM, OG reduced biofilm formation by approximately 59% and 84%, respectively, with BL irradiation for 15 min. These results confirmed that BL irradiation significantly enhanced the inhibitory effect of OG on *P. fluorescens* biofilm formation.

3D confocal scanning microscopy (CLSM) experiments using Live/Dead Baclight assay kit was performed to further elucidate the synergistic antibiofilm effect of OG and BL irradiation. The green-fluorescence nucleic acid stain SYTO 9 could enter into all (live and dead) bacterial cells in biofilms by penetrating. However, PI (red fluorescence) penetrates only dead bacteria with damaged membranes, generally causing a reduction in the SYTO 9 stain fluorescence (Jung, Wen, & Sun, 2019). Therefore, living bacteria with an intact membrane stain fluorescence green, whereas dead bacteria stain red when observed via CLSM. As shown in Fig. 3(C), compared with negative control (Fig. 3C-(a)) and positive controls (BL or OG alone) (Fig. 3C-(b), (c)), biofilms treated with OG+BL presented a large amount of red fluorescent spots (Fig. 3(C)-(d)~(f)), due to the highly active synergistic effect of OG and BL irradiation. Also, the inhibitory effect of 0.1 mM OG on

biofilm formation was similar to those treated by 0.05 mM OG coupled with BL irradiation (Fig. 3C-(d), (e)). These results were in good agreement with the findings in Fig. 3B.

[Fig. 3.]

3.5. Ablation effect of OG-mediated PDI on preformed biofilms of P. fluorescens

Apart from the excellent capability of inhibiting biofilm formation, the combination of OG and BL irradiation was capable of efficiently eradicating the mature biofilms. In Fig. 4A, approximately 8% and 4% (P<0.05) of biofilms were removed after treatment with 0.4 mM OG alone or BL irradiation, respectively, in comparison to the negative control. However, the performed biofilms submitted to OG-mediated PDI had a significant reduction, which ranged from 32% to 55%, depending on the dosage of BL irradiation. 3D CLSM (Fig. 4B) images confirmed that in the presence of BL irradiation, the eradication effect of OG was significantly enhanced. OG with BL irradiation for 90 min showed the highest biofilm-eradicating efficacy. More specifically, the biofilms of the control sample preserved the integrity of biofilm three-dimensional (3D) architectures and extracellular matrices (Fig. 4B-(a)). When evaluating BL irradiation alone and the OG in dark (Fig. 4B-(b), (c)), although a large number of colonies sustained green, some few were stained in red. However, following treatment with OG+BL, many bacterial cells disappeared throughout the biofilms (Fig. 4B-(d), (e), and (f)), indicating that the biofilms were very susceptible to OG-mediated PDI treatment. This qualitative assessment was consistent with quantitative data showing the biovolumes of biofilms in Fig. 6(A). There are numerous dead bacterial cells (red fluorescence cells) in biofilms treated by the combination of OG and 90 min BL irradiation (Fig. 4B-(f)), confirming that this treatment is substantially effective in eradicating mature bacterial biofilm together, these obtained results clearly indicate the excellent capability of OG+BL irradiation to eradicate existing biofilms and, therefore, leading to cell death. Cell viability in the treated biofilms further confirmed the enhanced effect, as mentioned above. In comparison with the samples treated with either OG or BL alone, the significant reduction of the number of viable bacteria in both the supernatant and biofilm caused by the synergistic action of OG and BL irradiation could be observed (Fig. 4C and D). Moreover, the viable count of bacteria was also reduced in an irradiation dosage-dependent manner and OG-mediated PDI for 90 min resulted in 68% and 79% reduction in supernatant and biofilm cells, respectively. Rocha et al. (2020) also found that PDI can reduce the number of colonies in the biofilm of *E. faecalis*. Our results revealed that OG-mediated PDI not only exhibited a robust inhibition of biofilm production and formation but also had a better effect on eradicating

581 the existing biofilms.

582

583 **[Fig. 4.]**

584 *3.6. Effect of a combination of OG/PLA NFs based packaging and PDI on giant salamander*
585 *preservation*

586 Electrospun nanofibers loaded with antimicrobial agents are excellent candidates for food
587 packaging materials to actively prevent food contamination during food storage. Following the
588 successful preparation of OG/PLA NFs, we then evaluated its PDI activity against *P. fluorescens*.
589 The results in Fig. 5A show that the combination of OG/PLA NFs and BL exposure could lead to
590 remarkable reductions in bacterial counts. The situ antibacterial activity of OG/PLA NFs based
591 packaging was evaluated during the Chinese giant salamander storge. Fig. 5B illuminates the total
592 viable count (TVC) of salamander meat during storage after selected treatments. The TVC of
593 control rose rapidly to 9.3 Log CFU/g after 15 days of storage. Conversely, samples packed with
594 OG/PLA NFs with or without BL irradiation have a lower initial bacterial count as described above,
595 and the number of colonies maintained at a low level (<2 Log CFU/g) during the storage especially
596 for the group treated with irradiation. The contaminated salamander meat was packed with OG/PLA
597 NFs under the BL exposure for 30 min, the bacterial count was reduced by ~99% and a great
598 reduction (80%) of viable bacterial counts could be observed as compared to the control after 15
599 days of storage. These findings further confirm that OG plays a dual role as an antibacterial agent
600 and photosensitizer to effectively mitigate foodborne pathogens. Moreover, The PCA region of
601 salamander meat packaged with OG/PLA NFs was the closest to the fresh sample than other ones
602 (Fig. 5C), suggesting that the OG/PLA NFs with BL exposure can exhibit robust antimicrobial
603 efficacy to effectively maintain the meat quality of salamander. These results indicated that
604 OG/PLA NFs as active food packaging material can prevent the contamination of foodborne
605 pathogens and efficiently improve the shelf life of fresh perishable food during storage.

606

607 **[Fig. 5.]**

608

609 **4. Conclusion**

610 In summary, this study demonstrated for the first time that the combination of OG at the lower
611 concentration and BL irradiation exerts notable synergistic bactericidal and biofilm ablation effects

against *P. fluorescens*. The dual roles of OG as a promising PS as well as an effective antibacterial agent has been highlighted in the OG-mediated PDI. We also elaborated the mechanism of synergistic bactericidal action by the simultaneous treatment with OG and BL irradiation that might be related to oxidative stress. And the process of ROS generation induced by OG-mediated PDI is more complex than originally thought, likely involving a specific interaction between OG and BL as well as between OG and ETC, especially exterior and interior •OH radicals. Furthermore, the electrospun nanofibers of OG/PLA were fabricated with excellent photodynamic antibacterial activity and also effectively reduced bacteria on the surface of the Chinese giant salamander. Therefore, our obtained excellent results also provide insights into the design and fabrication of future alternative antimicrobial and removing/reducing biofilm approaches that could be used in various situations associated with food sanitary.

Acknowledgments

The work was supported by the National Natural Science Foundation of China (21106131), Zhejiang Province Public Welfare Technology Application Research Project (LGJ19C200001), Academic Exchanges and Talent Training Program (2017SICR109), Zhejiang Provincial Program for Overseas High-Level Experts Introduction (Z20170407), as well as Food Science and Engineering the Most Important Discipline of Zhejiang Province (JYTsp20142101).

Abbreviation

Photodynamic inactivation, PDI
Light-emitting diode, LED
Blue light, BL
Photosensitizer, PS
Reactive oxygen species, ROS
Octyl gallate, OG
Gallic acid, GA
Hydrogen peroxide, H_2O_2
Hydroxyl radicals, •OH
Superoxide anion $\bullet O_2^-$
Electron transport chain, ETC
Total viable count, TVC
Pseudomonas fluorescens, *P. fluorescens*
Staphylococcus aureus, S. aureus

References

Akagawa, M., Shigemitsu, T., & Suyama, K. (2004). Production of hydrogen peroxide by polyphenols and polyphenol-rich beverages under quasi-physiological conditions. *Bioscience Biotechnology & Biochemistry, 67*(12), 2632–2640. https://doi.org/10.1271/bbb.67.2632.

Almeida, A., Faustino, M. AF., & Tomé, J. PC. (2015). Photodynamic inactivation of bacteria: Finding the effective targets. *Future Medicinal Chemistry, 7(10)*, 1221–1224. https://doi.org/10.4155/fmc.15.59.

Arakawa, H., Maeda, M., Okubo, S., & Shimamura, T. (2004). Role of hydrogen peroxide in bactericidal action of catechin. *Biological & Pharmaceutical Bulletin, 27*(3), 277–281. https://doi.org/10.1248/bpb.27.277.

Caldera, L., Franzetti, L., Van Coillie, E., De Vos, P., Stragier, P., De Block, J., & Heyndrickx, M. (2016). Identification, enzymatic spoilage characterization and proteolytic activity quantification of Pseudomonas spp. isolated from different foods. *Food Microbiology, 54*, 142-153. https://doi.org/10.1016/j.fm.2015.10.004.

Cebrian, G., Manas, P., & Condon, S. (2016). Comparative Resistance of Bacterial Foodborne Pathogens to Non-thermal Technologies for Food Preservation. *Front Microbiol, 7*, 734. https://doi.org/10.3389/fmicb.2016.00734.

Cossu, A., Ercan, D., Wang, Q., Peer, W. A., Nitin, N., & Tikekar, R. V. (2016). Antimicrobial effect of synergistic interaction between UV-A light and gallic acid against *Escherichia coli O157:H7* in fresh produce wash water and biofilm. *Innovative Food Science & Emerging Technologies, 37*, 44-52. https://doi.org/10.1016/j.ifset.2016.07.020.

Damiano, S., Forino, M., De, A., Vitali, L. A., Lupidi, G., & Taglialatela-Scafati, O. (2017). Antioxidant and antibiofilm activities of secondary metabolites from Ziziphus jujuba leaves used for infusion preparation. Food Chem, 230, 24-29. https://doi.org/10.1016/j.foodchem.2017.02.141.

D'Souza, C., Yuk, H.-G., Khoo, G. H., & Zhou, W. (2015). Application of Light-Emitting Diodes in Food Production, Postharvest Preservation, and Microbiological Food Safety. *Comprehensive Reviews in Food Science and Food Safety, 14*(6), 719-740. https://doi.org/10.1111/1541-4337.12155.

FDA. Code of Federal Regulations (CFR), 2001a. CFR (Code of Federal Regulations), Title 21: Food and Drugs. Chapter I e Food and Drug Administration, Department of Health and Human Services, Part 170 e Food Additives, Office of the Federal Register, Washington, DC (Revised April, 2008).

FDA. Code of Federal Regulations (CFR), 2001b. CFR (Code of Federal Regulations), Title 21: Food and Drugs. Chapter I e Food and Drug Administration, Department of Health and Human Services, Part 184 e Direct Food Substances affirmed as generally recognized as safe (GRAS), Office of the Federal Register, Washington, DC (Revised April, 2008).

Ferrario, M., Alzamora, S. M., & Guerrero, S. (2015). Study of the inactivation of spoilage microorganisms in apple juice by pulsed light and ultrasound. *Food Microbiol, 46*, 635-642. https://doi.org/10.1016/j.fm.2014.06.017.

Flemming, H. C., & Wingender, J. (2010). The biofilm matrix. *Nat Rev Microbiol, 8*(9), https://doi.org/623-633. 10.1038/nrmicro2415.

Huang, J., Chen, B., Li, H., Zeng, Q.-H., Wang, J. J., Liu, H., Pan, Y., & Zhao, Y. (2020). Enhanced antibacterial

and antibiofilm functions of the curcumin-mediated photodynamic inactivation against *Listeria monocytogenes*. *Food Control, 108*. https://doi.org/10.1016/j.foodcont.2019.106886.

Jung, J., Wen, J., & Sun, Y. (2019). Amphiphilic quaternary ammonium chitosans self-assemble onto bacterial and fungal biofilms and kill adherent microorganisms. *Colloids Surf B Biointerfaces, 174*, 1-8. https://doi.org/10.1016/j.colsurfb.

Kanno, T., Nakamura, K., Ikai, H., Hayashi, E., Shirato, M., Mokudai, T., Iwasawa, A., Niwano, Y., Kohno, M., Sasaki, K. (2012). Novel denture cleaning system based on hydroxyl radical disinfection. *Int. J. Prosthodont. 25*(4), 376−380.

Kayaci, F., & Uyar, T. (2012). Encapsulation of vanillin/cyclodextrin inclusion complex in electrospun polyvinyl alcohol (PVA) nanowebs: Prolonged shelf-life and high temperature stability of vanillin. *Food Chemistry, 133*(3), 641-649. https://doi.org/10.1016/j.foodchem.2012.01.040.

Kim, M. J., Mikš-Krajnik, M., Kumar, A., & Yuk, H. G. (2016). Inactivation by 405±5 nm light emitting diode on *Escherichia coli O157:H7*, *Salmonella Typhimurium*, and *Shigella sonnei* under refrigerated condition might be due to the loss of membrane integrity. *Food Control, 59*, 99-107. https://doi.org/10.1016/j.foodcont.2015.05.012.

Kim, M. J., Bang, W. S., & Yuk, H. G. (2017). 405 +/- 5 nm light emitting diode illumination causes photodynamic inactivation of Salmonella spp. on fresh-cut papaya without deterioration. *Food Microbiol, 62*, 124-132. https://doi.org/10.1016/j.fm.2016.10.002.

Kubo, I., Fujita, K., Nihei, K., & Nihei, A. (2004). Antibacterial activity of alkyl gallates against bacillus subtilis. *J Agric Food Chem, 52*(5), 1072–1076. https://doi.org/10.1021/jf034774l.

Luksienė, Z., & Zukauskas, A. (2009). Prospects of photosensitization in control of pathogenic and harmful micro-organisms. *J Appl Microbiol, 107*(5), 1415-1424. https://doi.org/10.1111/j.1365-2672.2009.04341.x.

Maclean, M., MacGregor, S. J., Anderson, J. G., & Woolsey, G. (2009). Inactivation of bacterial pathogens following exposure to light from a 405-nanometer light-emitting diode array. *Appl Environ Microbiol, 75*(7), 1932-1937. https://doi.org/10.1128/AEM.01892-08.

Mochizuki, M.; Yamazaki, S.; Kano, K.; Ikeda, T. (2002). Kinetic analysis and mechanistic aspects of autoxidation of catechins. *Biochim. Biophys. Acta, 1569*, 35−44. https://doi.org/10.1016/S0304-4165(01)00230-6.

Nakamura, K., Ishiyama, K., Sheng, H., Ikai, H., Kanno, T., & Niwano, Y. (2015). Bactericidal Activity and Mechanism of Photoirradiated Polyphenols against Gram-Positive and -Negative Bacteria. *J Agric Food Chem, 63*(35), 7707-7713. https://doi.org/10.1021/jf5058588.

Nakamura, K., Shirato, M., Ikai, H., Kanno, T., Sasaki, K., Kohno, M., & Niwano, Y. (2013). Photo-irradiation of proanthocyanidin as a new disinfection technique via reactive oxygen species formation. *PLoS ONE, 8*(3), e60053. https://doi.org/10.1371/journal.pone.0060053.

Nakamura, K., Shirato, M., Kanno, T., Lingstrom, P., Ortengren, U., & Niwano, Y. (2017). Photo-irradiated caffeic acid exhibits antimicrobial activity against *Streptococcus mutans* biofilms via hydroxyl radical formation. *Sci Rep, 7*(1), 6353. https://doi.org/10.1038/s41598-017-07007-z.

Nakamura, K., Yamada, Y., Ikai, H., Kanno, T., Sasaki, K., & Niwano, Y. (2012). Bactericidal action of photoirradiated gallic acid via reactive oxygen species formation. *J Agric Food Chem, 60*(40), 10048-10054.

https://doi.org/10.1021/jf303177p.

Nilsson, R. E., Ross, T., & Bowman, J. P. (2011). Variability in biofilm production by *Listeria monocytogenes* correlated to strain origin and growth conditions. *Int J Food Microbiol, 150*(1), 14-24. https://doi.org/10.1016/j.ijfoodmicro.2011.07.012.

Ortega-Rivas, E., & Salmeron-Ochoa, I. (2014). Nonthermal food processing alternatives and their effects on taste and flavor compounds of beverages. *Crit Rev Food Sci Nutr, 54*(2), 190-207. https://doi.org/10.1080/10408398.2011.579362.

Park, H. J., Kim, J. Y., Kim, J., Lee, J. H., Hahn, J. S., Gu, M. B., & Yoon, J. (2009). Silver-ion-mediated reactive oxygen species generation affecting bactericidal activity. *Water Res, 43*(4), 1027-1032. https://doi.org/10.1016/j.watres.2008.12.002

Rapacka-Zdonczyk, A., Wozniak, A., Pieranski, M., Woziwodzka, A., Bielawski, K. P., & Grinholc, M. (2019). Development of *Staphylococcus aureus* tolerance to antimicrobial photodynamic inactivation and antimicrobial blue light upon sub-lethal treatment. *Scientific Reports, 9*(1). https://doi.org/10.1038/s41598-019-45962-x.

Seo, H. J., & Kang, S. S. (2020). Inhibitory effect of bacteriocin produced by *Pediococcus acidilactici* on the biofilm formation of *Salmonella Typhimurium*. *Food Control, 117*. https://doi.org/10.1016/j.foodcont.2020.107361.

Sheng, L., Zhang, Z., Sun, G., & Wang, L. (2020). Light-driven antimicrobial activities of vitamin K3 against *Listeria monocytogenes*, *Escherichia coli O157:H7* and *Salmonella Enteritidis*. *Food Control, 114*, 107235. https://doi.org/10.1016/j.foodcont.2020.107235.

Shi, Y. G., Zhang, R. R., Zhu, C. M., Liang, X. R., Ettelaie, R., Jiang, L., & Lin, S. (2021). On the mechanism behind enhanced antibacterial activity of alkyl gallate esters against foodborne pathogens and its application in Chinese icefish preservation. *Food Microbiology, 99*. https://doi.org/10.1016/j.fm.2021.103817.

Shi, Y. G., Zhang, R. R., Zhu, C. M., Xu, M. F., Gu, Q., Ettelaie, R., Lin, S., Wang, Y. F., & Leng, X. Y. (2020). Antimicrobial mechanism of alkyl gallates against *Escherichia coli* and *Staphylococcus aureus* and its combined effect with electrospun nanofibers on Chinese Taihu icefish preservation. *Food Chem, 346*, 128949. https://doi.org/10.1016/j.foodchem.2020.128949.

Shi, Y. G., Zhu, Y. J., Shao, S. Y., Zhang, R. R., Wu, Y., Zhu, C. M., Liang, X. R., & Cai, W. Q. (2018). Alkyl Ferulate Esters as Multifunctional Food Additives: Antibacterial Activity and Mode of Action against *Escherichia coli* in Vitro. *J Agric Food Chem, 66*(45), 12088-12101. https://doi.org/10.1021/acs.jafc.8b04429.

Stiefel, P., Schmidt-Emrich, S., Maniura-Weber, K., & Ren, Q. (2015). Critical aspects of using bacterial cell viability assays with the fluorophores SYTO9 and propidium iodide. *BMC Microbiol, 15*, 36. https://doi.org/10.1186/s12866-015-0376-x.

Wang, Q., de Oliveira, E. F., Alborzi, S., Bastarrachea, L. J., & Tikekar, R. V. (2017). On mechanism behind UV-A light enhanced antibacterial activity of gallic acid and propyl gallate against *Escherichia coli O157:H7*. *Sci Rep, 7*(1), 8325. https://doi.org/10.1038/s41598-017-08449-1.

Wang, Q., Leong, W. F., Elias, R. J., & Tikekar, R. V. (2019). UV-C irradiated gallic acid exhibits enhanced antimicrobial activity via generation of reactive oxidative species and quinone. *Food Chem, 287*, 303-312.

https://doi.org/10.1016/j.foodchem.2019.02.041.

Wen, P., Wen, Y., Zong, M. H., Linhardt, R. J., & Wu, H. (2017). Encapsulation of Bioactive Compound in Electrospun Fibers and Its Potential Application. *J Agric Food Chem, 65*(42), 9161-9179. https://doi.org/10.1021/acs.jafc.7b02956.

Zhang, R. R., Shi, Y. G., Gu, Q., Fang, M., Chen, Y. W., Fang, S., Dang, Y. L., & Chen, J. S. (2021). Antimicrobial effect and mechanism of non-antibiotic alkyl gallates against *Pseudomonas fluorescens* on the surface of Russian sturgeon (Acipenser gueldenstaedti). *Int J Food Microbiol, 342*, 109093. https://doi.org/10.1016/j.ijfoodmicro.2021.109093.

TABLES and FIGURE Legends

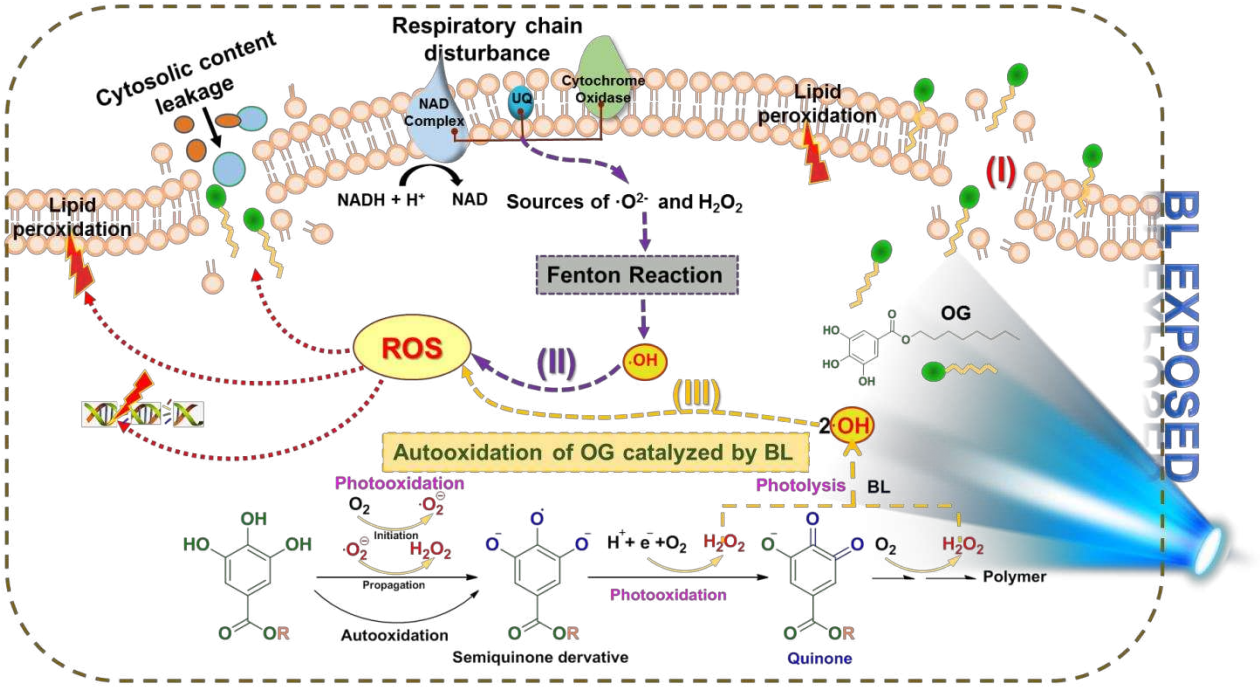

Scheme 1. Proposed mechanism of the OG-mediated photodynamic inactivation against *P. fluorescens*. (I) OG damages the membrane of bacterial cells and easily permeates into the intact cells and then (II) disrupts the activity of ETC on the cytoplasmic membrane to generate a high level of toxic ROS. (III) The polyphenolic hydroxyl group of OG would be oxidized by the photoradiation of BL to generate •OH. As a consequence, these ROS-triggered damages lead to microbial cell inactivation and death due to damage to intracellular molecules, such as the essential proteins, DNA, and lipids.

781 **Figures**

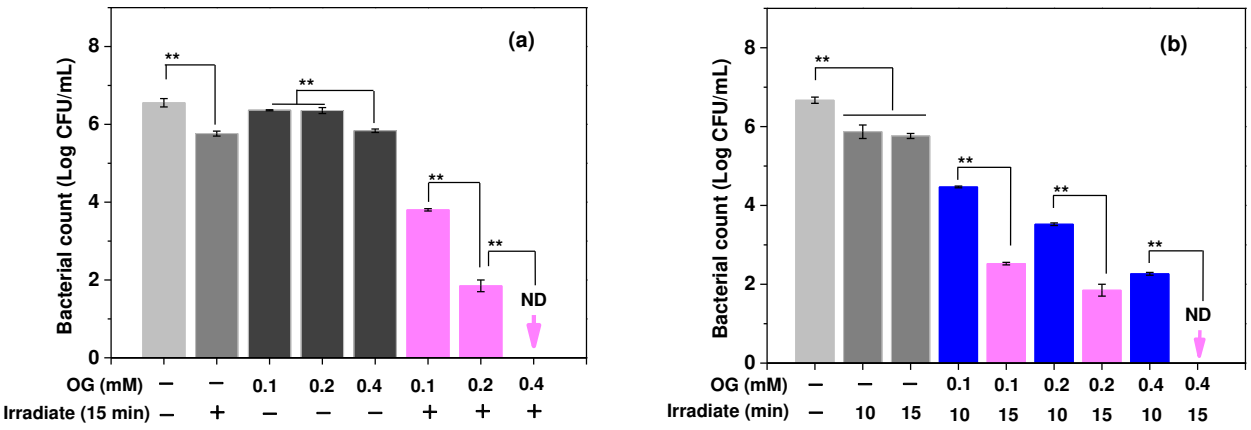

(A)

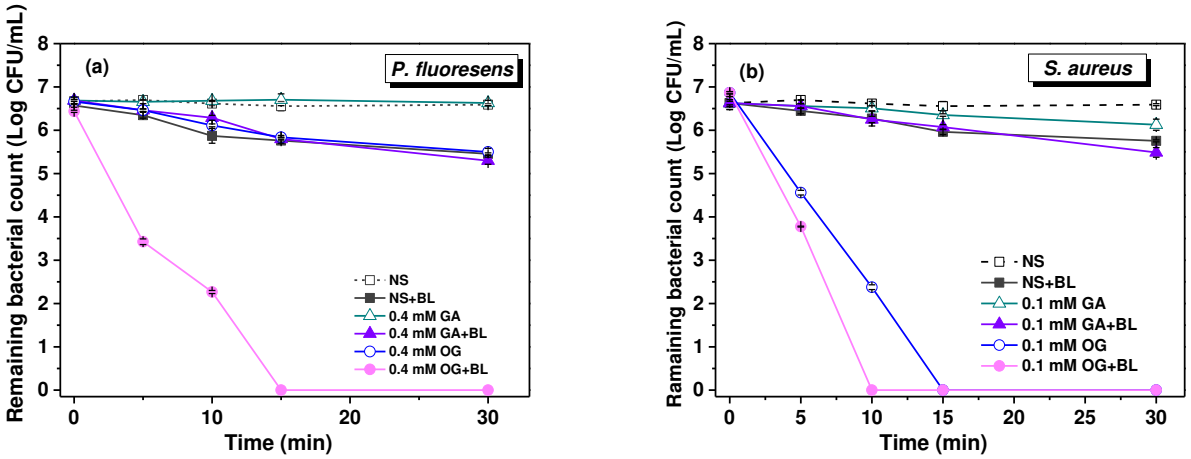

(B)

782

783 **Fig. 1**. (**A**) Evaluate the effect of OG or GA concentration and BL irradiation time on the
784 antimicrobial activity against *P. fluorescens* in the absence or presence of BL irradiation at 25 ºC.
785 The number of bacteria in the suspension was determined by standard plate counting (Wavelength:
786 420 nm, irradiance: 212 mW/cm^2). (**a**) OG concentration-dependent bactericidal activity. (**b**) The
787 effect of irradiation time on the bactericidal activity of OG-mediated PDI. (**B**) Time-dependent
788 bactericidal activity against (**a**) *P. fluorescens* and (**b**) *S. aureus* (wavelength: 420 nm, irradiance:
789 212 mW/cm^2). Values and error bars indicate the mean and standard deviation, respectively.
790 Significant differences are shown, P<0.05 (*) and P<0.01 (**). ND: not detected. OG: octyl gallate,
791 GA: gallic acid, OG, NS: normal saline.

792

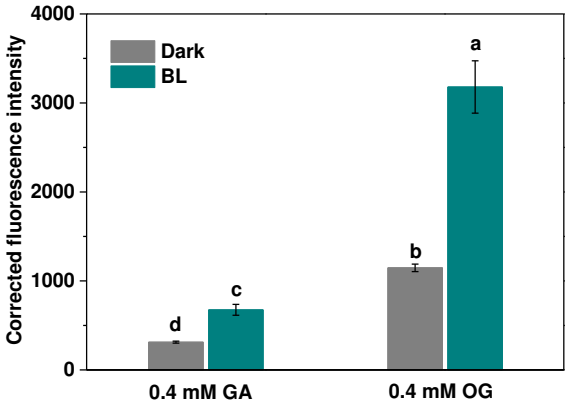
Corrected fluorescence intensity
4000
3000
2000
1000
0
Dark
BL
a
b
c
d
0.4 mM GA
0.4 mM OG

(A)

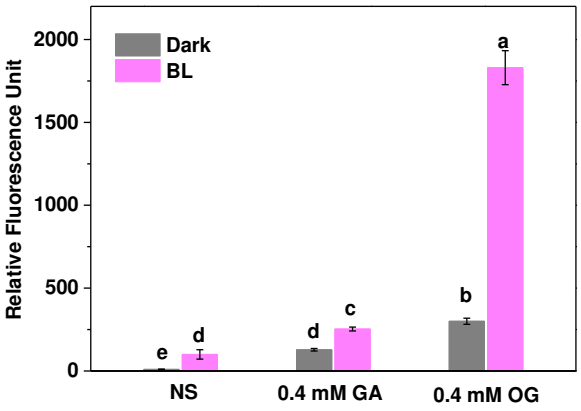
Relative Fluorescence Unit
2000
1500
1000
500
0
Dark
BL
a
b
c
d
e
NS
0.4 mM GA
0.4 mM OG

(B)

793

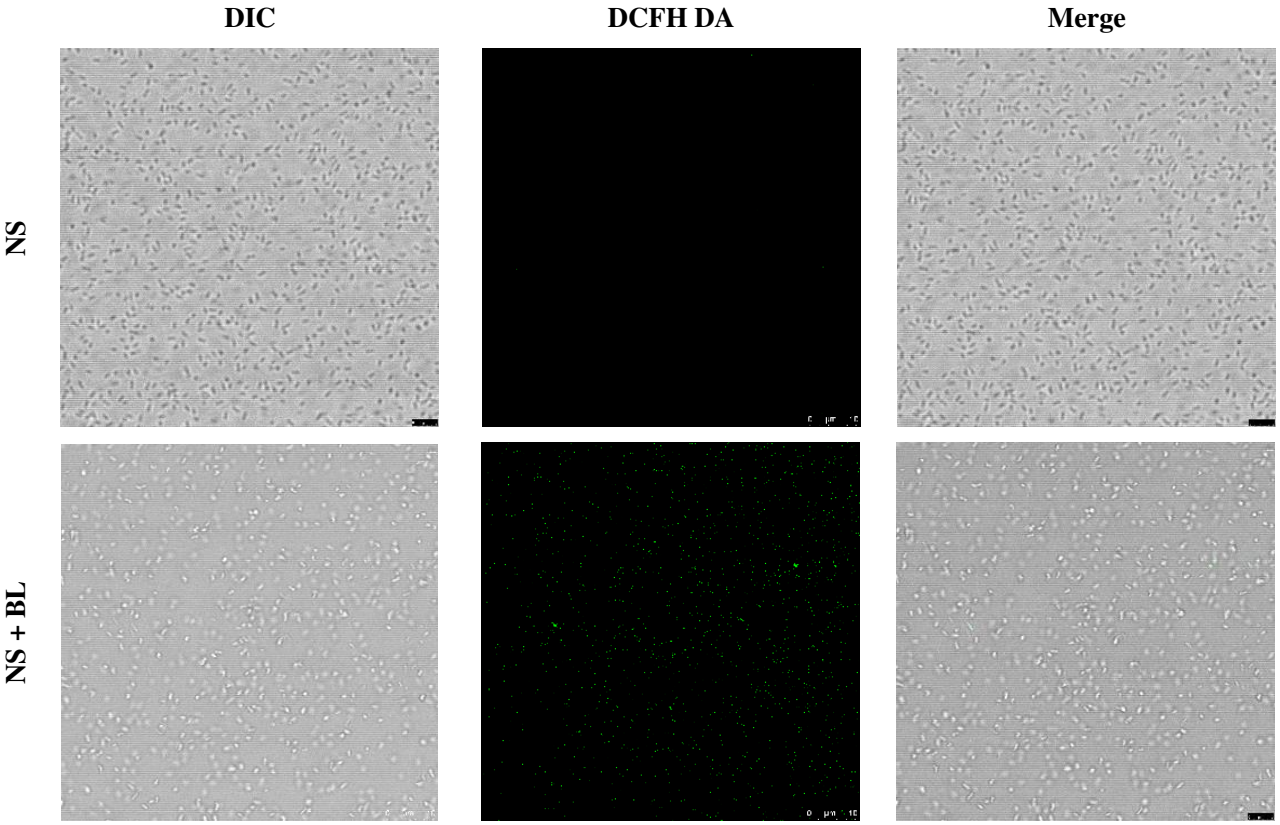
DIC
DCFH DA
Merge
NS
NS + BL

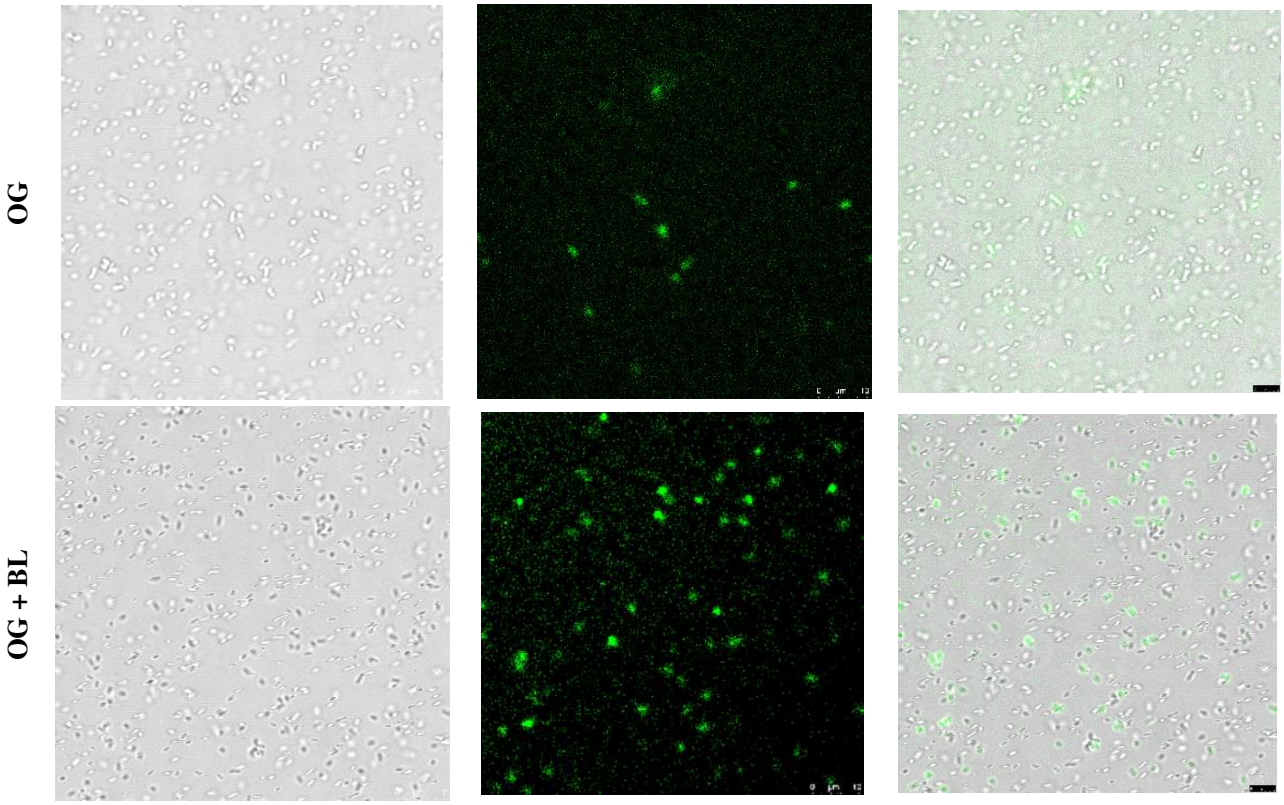
OG
OG + BL

(C)

794

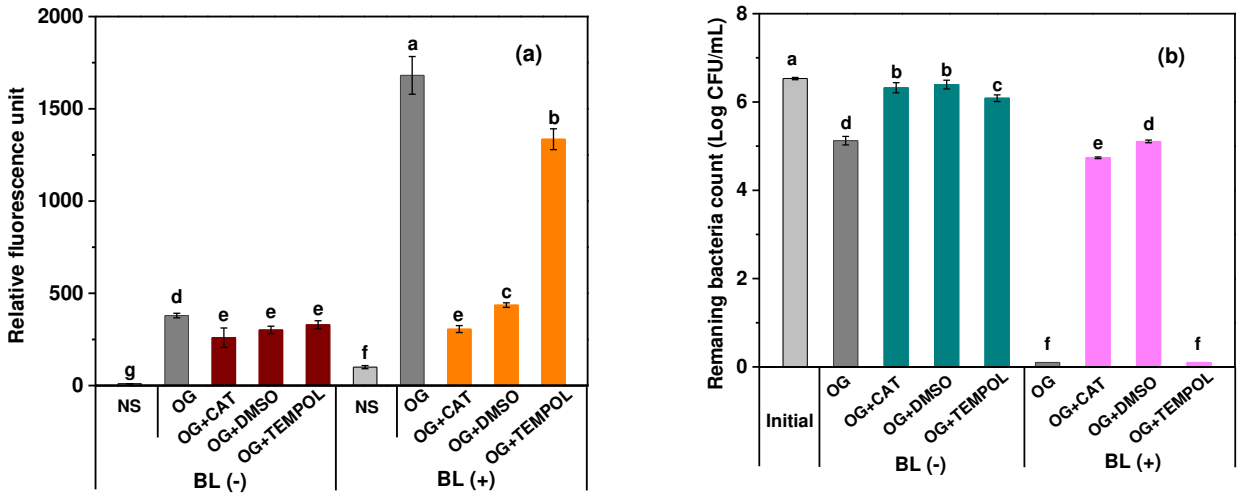
Relative fluorescence unit
2000
1500
1000
500
0
(a)
g
d
e
e
e
f
a
e
c
b
NS
OG
OG+CAT
OG+DMSO
OG+TEMPOL
NS
OG
OG+CAT
OG+DMSO
OG+TEMPOL
BL (-)
BL (+)
Remaning bacteria count (Log CFU/mL)
8
6
4
2
0
(b)
a
d
b
b
c
f
e
d
f
Initial
OG
OG+CAT
OG+DMSO
OG+TEMPOL
OG
OG+CAT
OG+DMSO
OG+TEMPOL
BL (-)
BL (+)

(D)

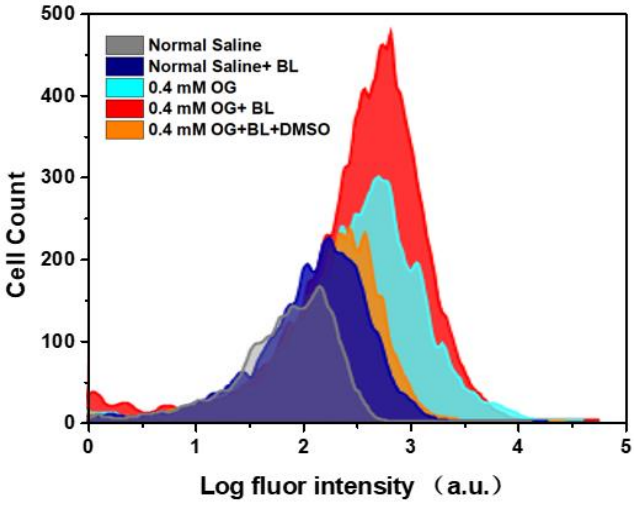

(E)

795

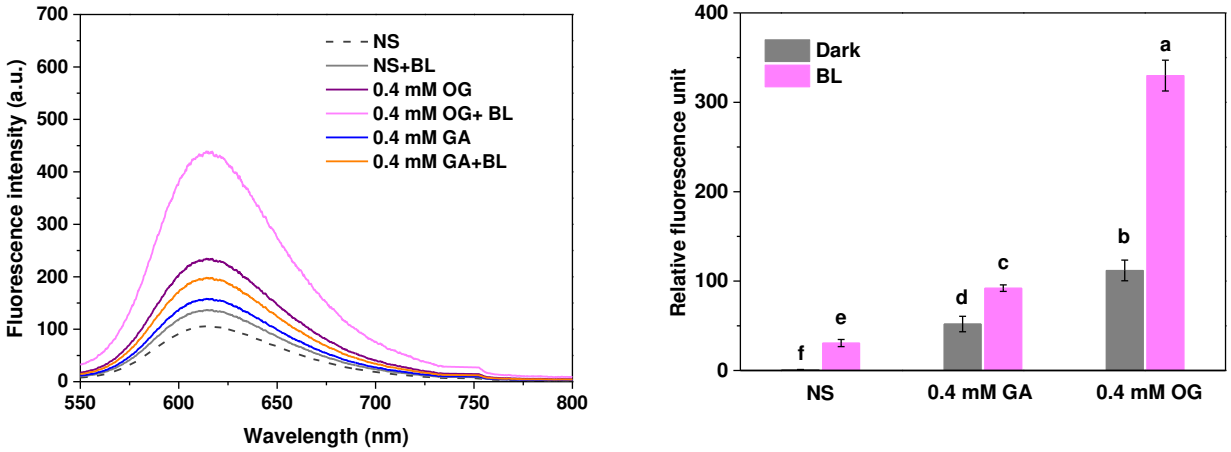

(F)

796

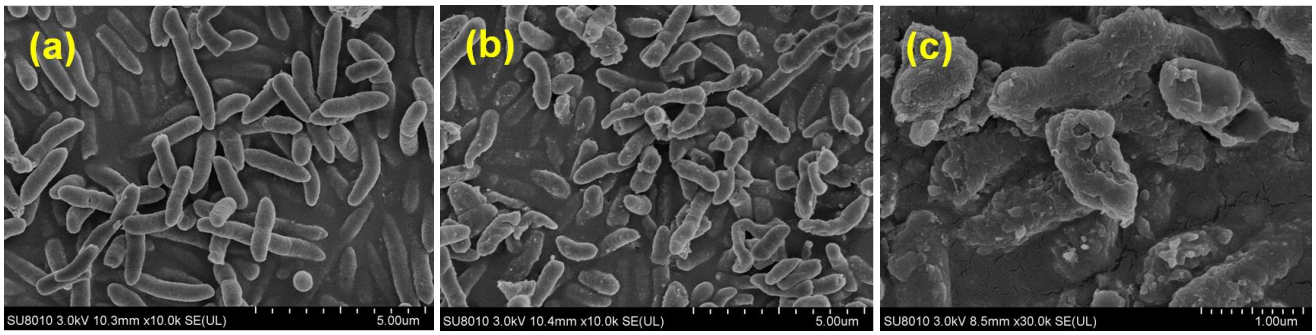

(G)

797

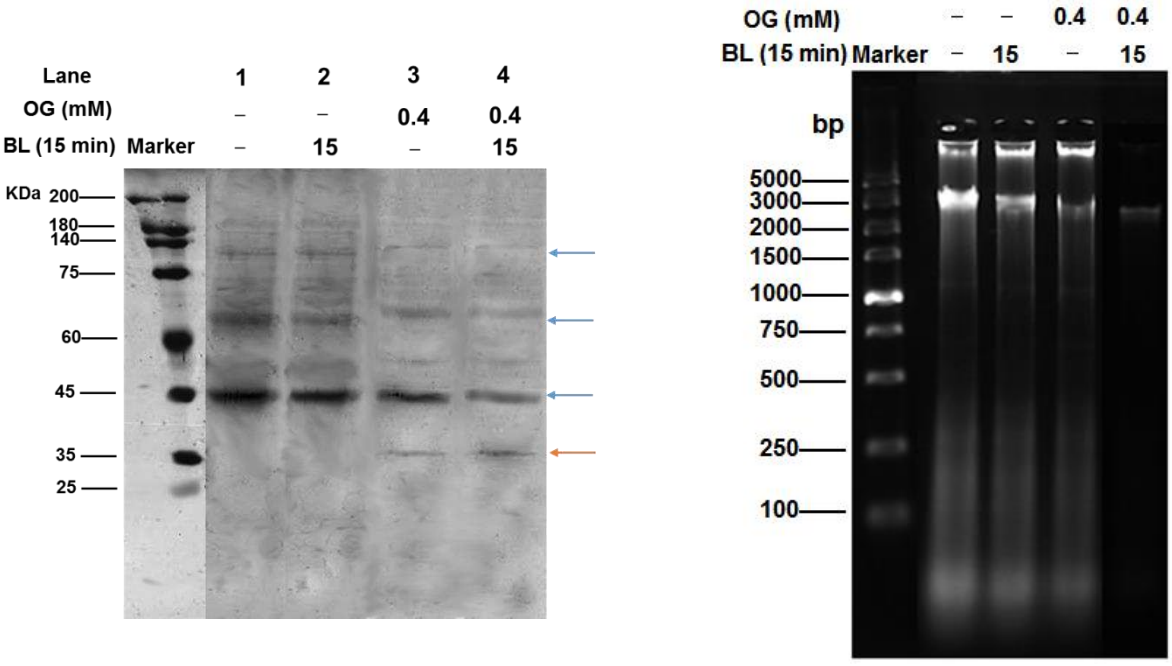

(H) **(I)**

Fig. 2. (**A**) Measurement of uptake of OG or GA in *P. fluoresens* using fluorescent-based indicators diphenylboric acid 2-aminoethyl ester (DPBA). *P. fluorescens* treated by OG or GA solution (0.4 mM) in the presence and absence of BL irradiation for 30 min. Absolute fluorescence values were corrected by subtracting the fluorescence values for samples incubated in water and in dark. (**B**) Total reactive oxygen species (ROS) were detected using DCFH-DA in *P. fluorescens* treated by OG (0.4 mM) solution in the presence and absence of BL. (**C**) CLSM images of *P. fluorescens* incubated with DCFH-DA. Photodynamic inactivation of *P. fluorescens* was evaluated at 30 °C in presence of OG (0.4 mM) and simultaneously illuminated by BL for 20 min (DIC-differential interference contrast). The initial bacterial density of *P. fluorescens* is ~8 Log CFU/mL. Pictures were taken using ×63 oil immersion lens with a zoom factor of 2. (**D**) (**a**) Detection of intracellular reactive oxygen species (ROS) using DCFH-DA within *P. fluorescens* with or without scavengers including CAT (1200 U/mL), DMSO (2.8 M), or TEMPOL (16 mM). (**b**) Antibacterial assessments of OG alone or OG-mediated PDI with or without CAT (1200 U/mL), DMSO (2.8 M), or TEMPOL (16 mM). The mixture of bacterial suspension and OG solution (0.4 mM) was irradiated with BL for 20 min. (**E**) Generation of hydroxyl radicals in *P. fluorescens* treated by OG (0.4 mM) solution in the presence and absence of BL irradiation. Values and error bars indicate the mean and standard deviation, respectively. Significant differences (P<0.05) between the groups are denoted by different superscript letters. (**F**) Membrane damage as indicated by the fluorescence level of PI in *P. fluorescens* treated by OG or GA solution with the final concentration of 0.4 mM in the presence and absence of BL irradiation (wavelength: 420 nm, irradiance: 212 mW/cm^2, treatment time: 20

819 min). The initial bacterial density of *P. fluorescens* is ~8 Log CFU/mL. (**G**) Scanning electron
820 microscopy (SEM) images of *P. fluorescens*. (a), (b) and (c) were SEM images of control, treatment
821 by 0.4 mM OG and 0.4 OG+BL for 20 min, respectively. (**H**) Effects of the OG+BL treatment on
822 the total protein of *P. fluorescens* treated by OG (0.4 mM) solution in the presence and absence of
823 BL irradiation. (**I**) Effects of the OG-mediated PDI on the genomic DNA of *P. fluorescens*. *P.*
824 *fluorescens* was treated by OG (0.4 mM) solution in the presence and absence of BL irradiation.
825 Values and error bars indicate the mean and standard deviation, respectively. Significant differences
826 (P<0.05) between the groups are denoted by different superscript letters.
827
828

829

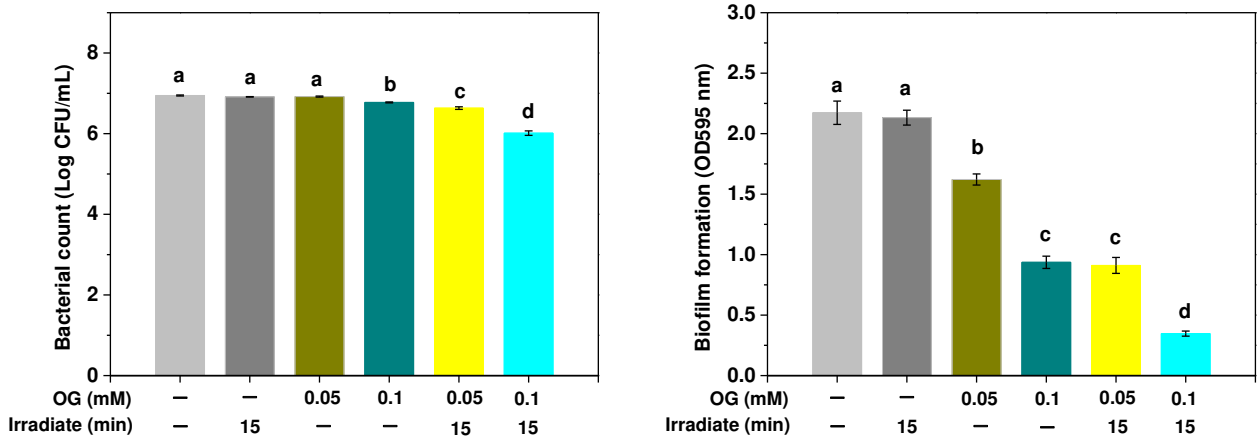

(A) (B)

830

	SYTO 9	PI	Merge
(a) OG(-)BL(-)	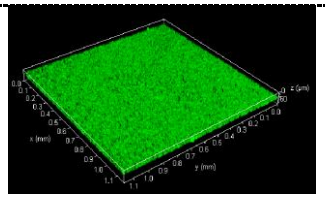	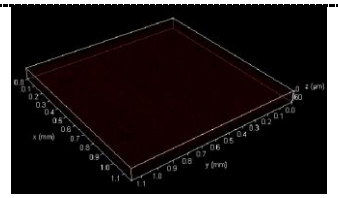	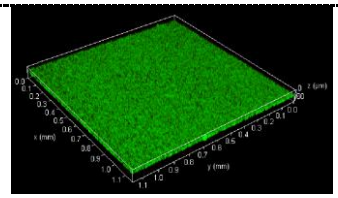
(b) OG(-)BL(+)	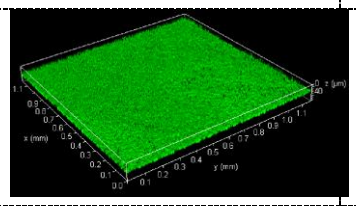	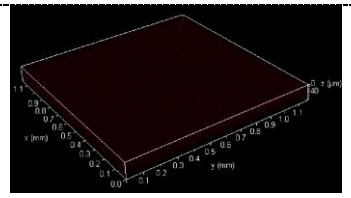	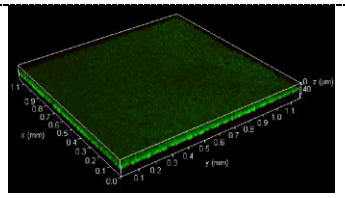
(c) 0.05 mM OG(+)BL(-)	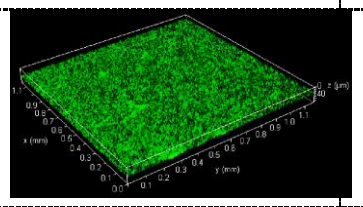	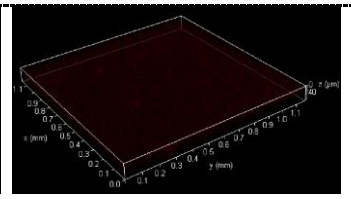	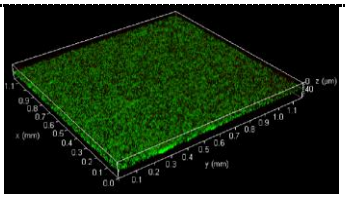
(d) 0.1 mM OG(+)BL(-)	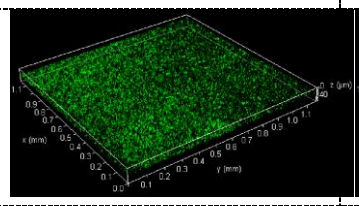	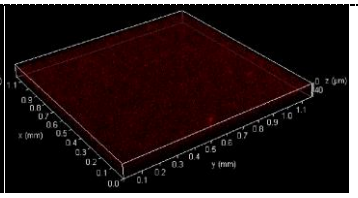	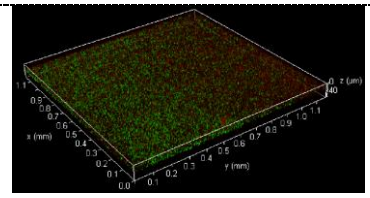
(e) 0.05 mM OG(+)BL(+)	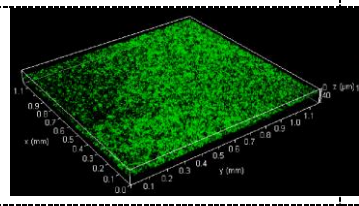	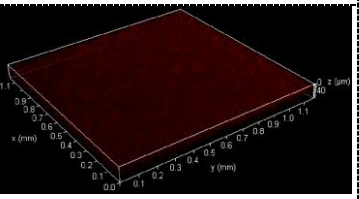	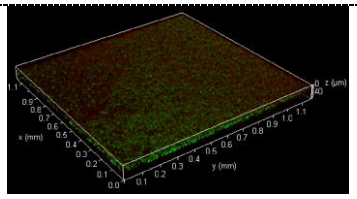

(f) 0.1 mM OG(+)BL(+)	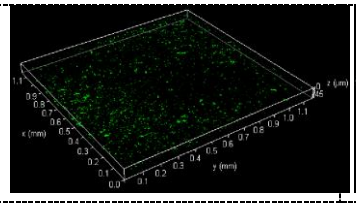	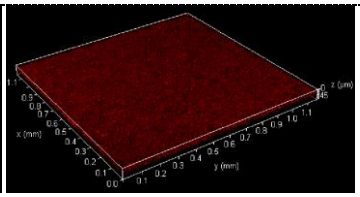	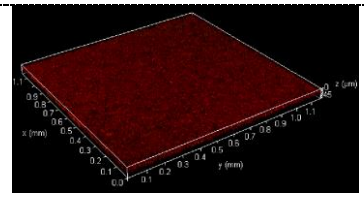

(**C**)

Fig. 3. Effect of OG coupled with BL irradiation on biofilm formation. (**A**) Surviving planktonic cells in the culture supernatant treated with OG in the absence or presence of BL irradiation for 15 min (wavelength 420 nm, irradiance: 94.8 mW/cm^2). (**B**) Relative biofilm formation for 60 h and (**C**) 3D CLSM images of *P. fluorescens* biofilms after different conditions. (**a**) The untreated control was further incubated for 60 h without OG and BL irradiation. (**b**) *P. fluoresens* were treated with BL irradiation alone for 15 min and further incubated for 60 h. (**c**) *P. fluoresens* were treated with 0.05 mM or (**d**) 0.1 mM OG alone for 15 min and further incubated for 60 h. (**e**) *P. fluoresens* were treated with 0.05 mM OG or 0.1 mM OG (**f**) combined with BL irradiation for 15 min and further incubated for 60 h. The first and second columns display bacteria labeled with LIVE/DEAD BacLight SYTO 9 (green) and PI (red) and the third column displays the merged pictures. Values and error bars indicate the mean and standard deviation, respectively. Significant differences (P<0.05) between the groups are denoted by different superscript letters.

846
847

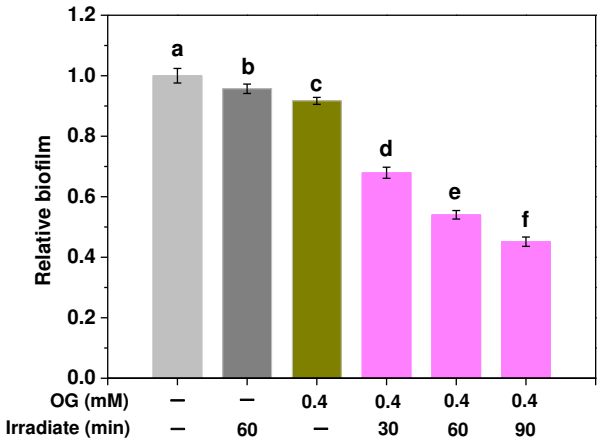

(A)

848

	SYTO 9	PI	Merged
(a) OG(-)BL(-) Control	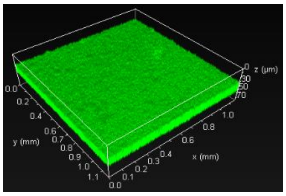	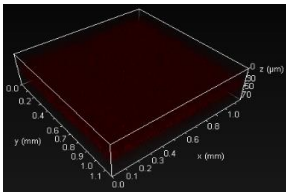	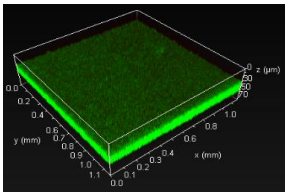
(b) OG(-)BL(+)	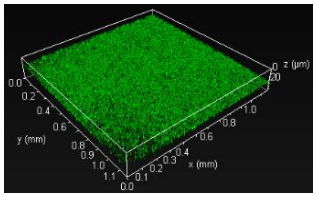	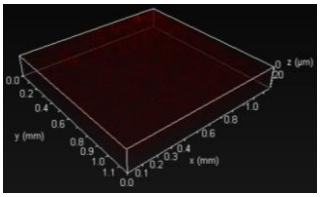	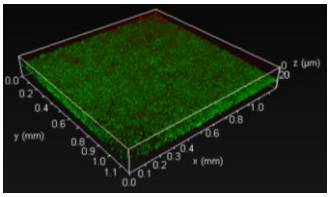
(c) OG(+)BL(-)	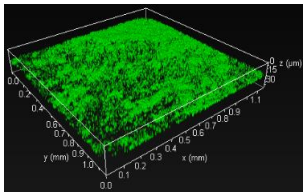	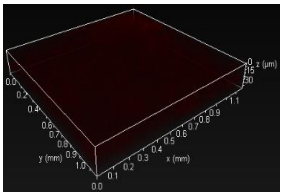	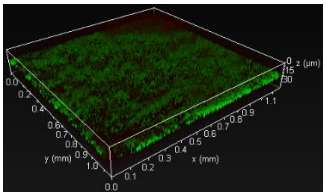
(d) OG(+)BL(+) 30 min	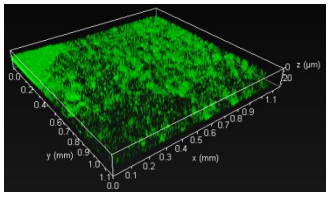	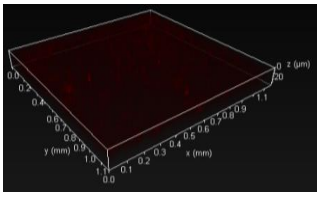	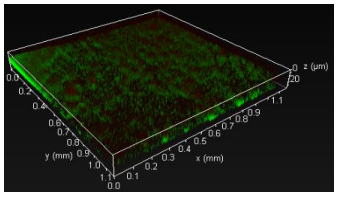

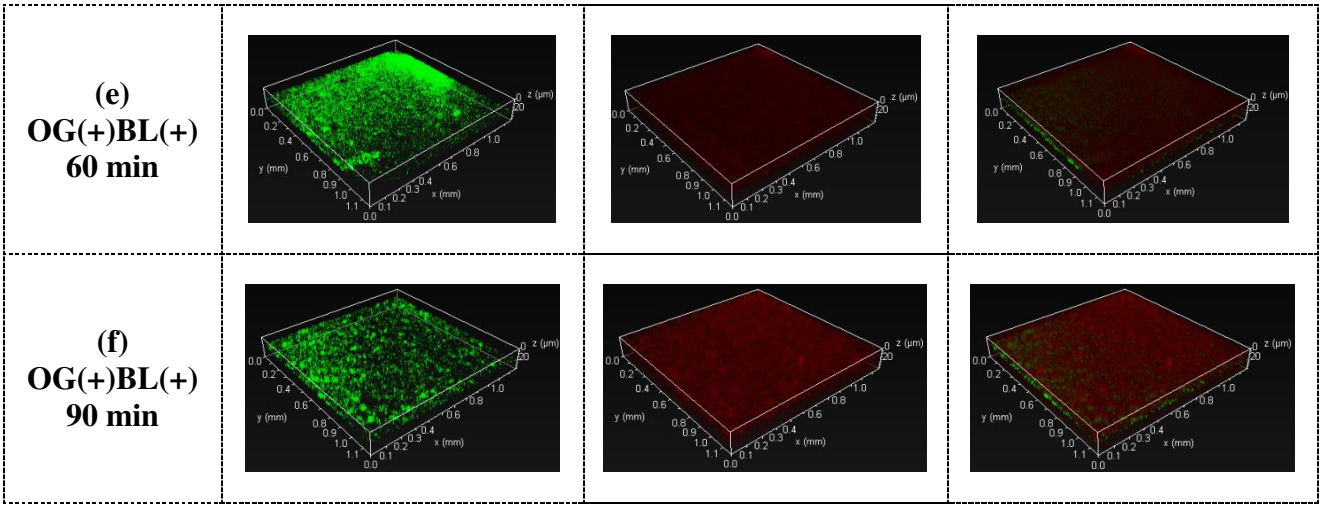

(**B**)

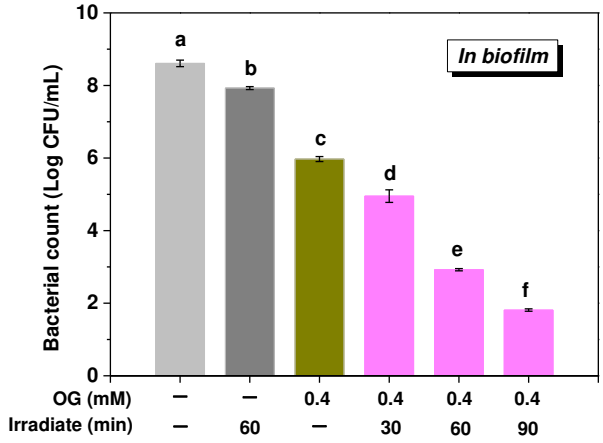

(**C**)

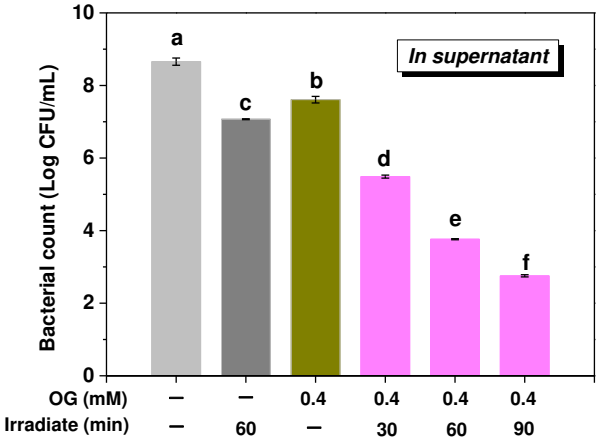

(**D**)

Fig. 4. Effect of OG+BL on preformed biofilms (wavelength 420 nm, irradiance: 212 mW/cm^2). (**A**) Relative biofilm. (**B**) 3D CLSM images of *P. fluoresens* biofilms after different treatments. (**a**) The untreated control constituted a 60 h-old biofilm further cultivated for 60 min without OG and BL irradiation. (**b**) *P. fluoresens* 60 h-old biofilms were treated with BL irradiation alone for 60 min. (**c**) *P. fluoresens* 60 h-old biofilms were treated with 0.4 mM OG for 60 min. (**d**) *P. fluoresens* 60 h-old biofilms were treated with 0.4 mM OG coupled with BL irradiation for different exposure times (**d**) 30 min, (**e**) 60 min, and (**f**) 90 min. The first and second columns display bacteria labeled with LIVE/DEAD BacLight SYTO 9 (green) and PI (red) and the third column displays the merged pictures. (**C**) Quantitative analysis of surviving cells in biofilms or (**D**) in the culture supernatant. Values and error bars indicate the mean and standard deviation, respectively. Significant differences (P<0.05) between the groups are denoted by different superscript letters.

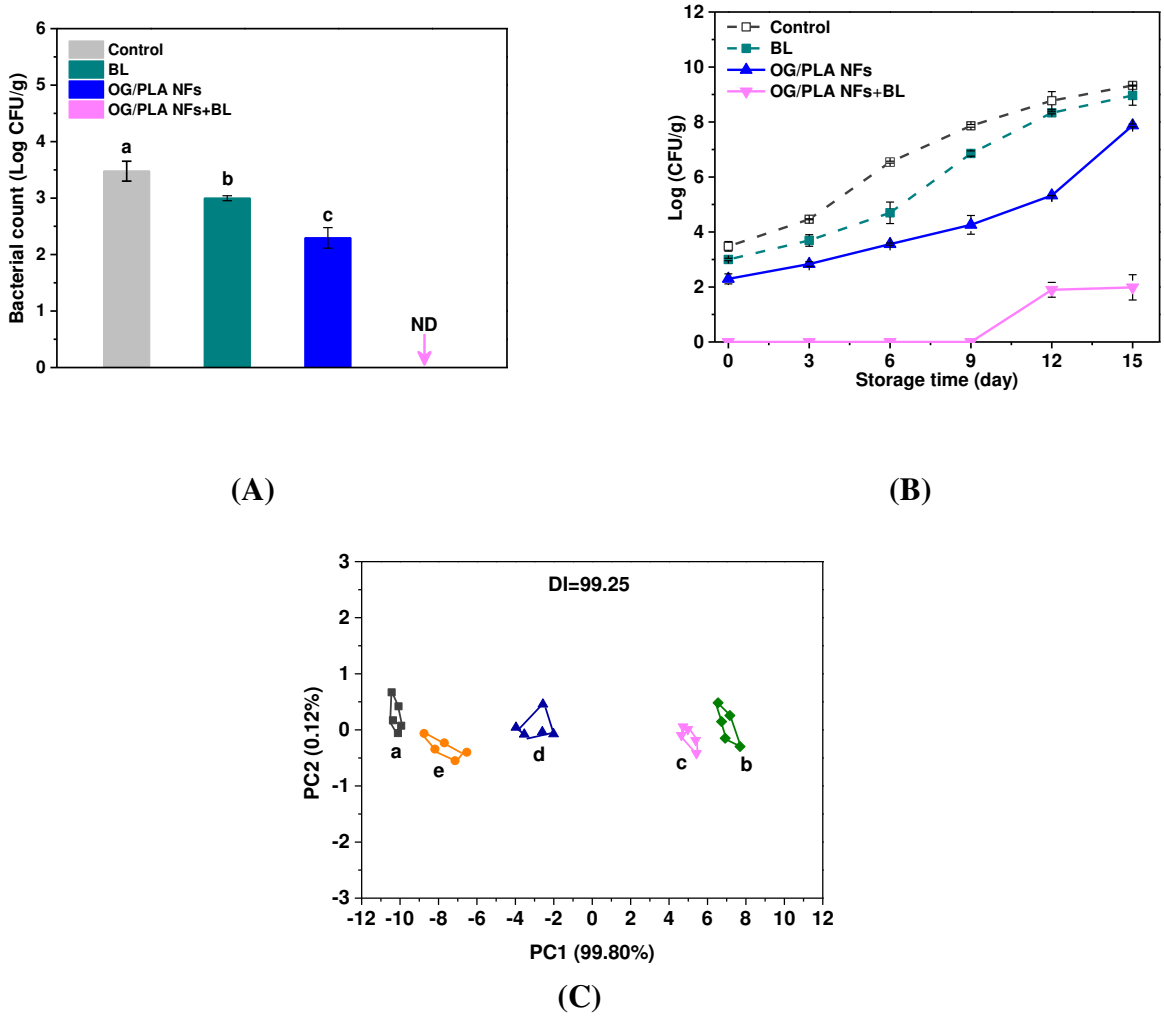

Fig. 5. The changes in preservation quality indices of Chinese giant salamander during storage at 4 ◦C. (**A**) Results of bactericidal assessments of OG/PLA NFs combined with BL irradiation against 3 Log CFU/mL bacteria. ND: not detected. (**B**) The change of colonies of Chinese giant salamander during the storage for 3, 6, 9, 12 and 15 days at 4 °C. The fresh salamander meat was packed using OG/PLA NFs and then immediately treated with BL irradiation for 30 min. (**C**) The PCA of Chinese giant salamander with different treatments: (**a**) fresh salamander meat; (**b**) control; (**c**) control+BL; (**d**) OG/PLA NFs; (**e**) OG/PLA+BL; (b-e, 4 °C, 15 days). The salamander meats were singly sealed with OG/PLA NFs and irradiated immediately with BL for 30 min at a distance of 1 cm. Significant differences (P<0.05) between the groups are denoted by different letters.

875 **TOC GRAPHIC**

876

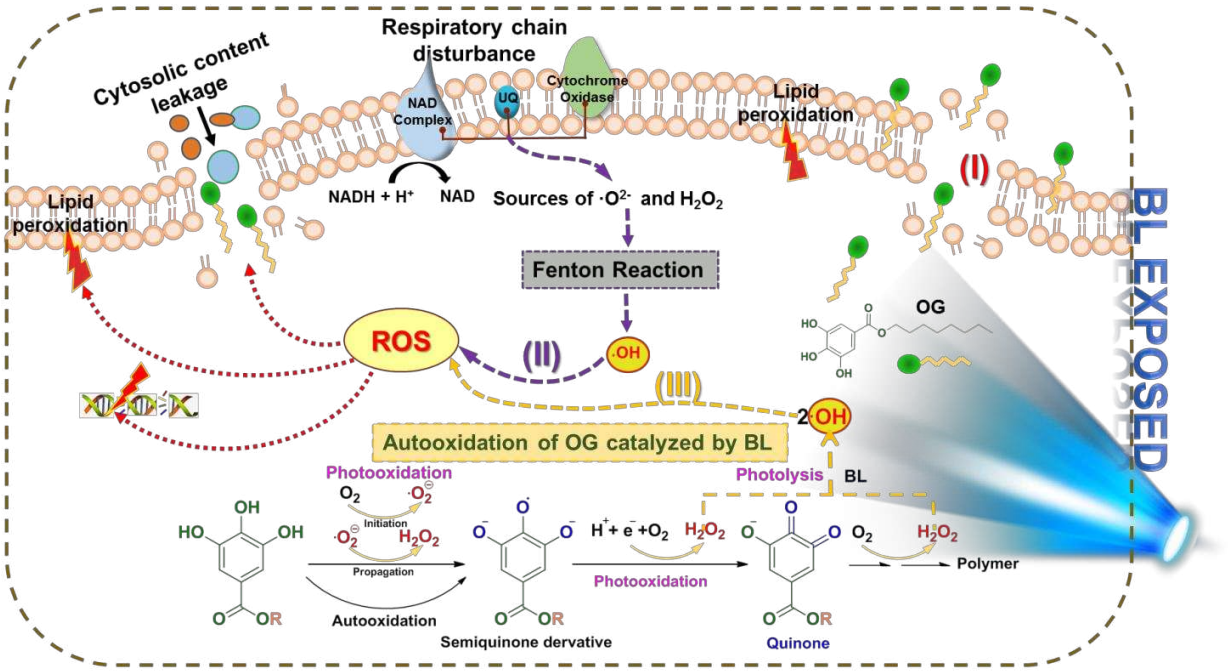

877

Supplementary Material
Click here to access/download;Supplementary Material;20210807 Supporting Info.docx

Submit online to *Food Chemistry*

Manuscript Number:

Title

Ultra-efficient photodynamic inactivation system based on blue light and alkyl gallate for synergistic antibacterial and ablation biofilms against *Pseudomonas fluorescens* and smart application with electrospun nanofibers on Chinese giant salamander preservation

Yu-gang Shi [a,b], Lai Jiang [a,b], Shan Lin [a,b], Wen-gang Jin [c], Qing Gu [a,b], Yue-wen Chen [a,b], Ke Zhang [a,b], Rammile Ettelaie [d]

[a] School of Food Science and Biotechnology, Zhejiang Gongshang University, Hangzhou, Zhejiang 310035, China
[b] Institute of Food Microbiology, Zhejiang Gongshang University, Hangzhou, Zhejiang 310035, China
[c] *Bio-resources Key Laboratory of Shaanxi Province, School of Biological Science and Engineering, Shaanxi University of Technology, Hanzhong 723001, China*
[d] *School of Food Science and Nutrition, University of Leeds, Leeds, LS2 9JT, UK*

Corresponding Author:

Yu-gang Shi
School of Food Science and Biotechnology, Zhejiang Gongshang University, Xiasha University Town, Xuezheng Str. 18, Hangzhou 310018, China
Tel.: 86-0571-28008927
E-mail: yugangshi@zjgsu.edu.cn

SURPPORTING INFORMATION

1. Method

1.1. Quantification of phenolics adsorption through CLSM

Quantification of phenolics (OG or GA) adsorption was conducted according to the method reported by Wang et al. (2017) with some modifications. The *P. fluorescens* cells were cultured in LB broth at 30 ºC for 14-16 h. The bacterial cells were harvested and washed three times with PBS (0.1 M, pH=7.2). Then the bacterial cells were resuspended in PBS to 8 Log CFU/mL and phenolics were added to the resuspension solution to a final concentration of 0.1 mM. Cells were incubated at 30 ºC for 30 min and then harvested. For the quantification of phenolics adsorption, 450 μL of DPBA solution (DMSO, 0.2% w/v) was added to the above bacterial cells and then incubated for 5 min. The images of the cells were captured using confocal laser scanning microscopy (CLSM, Leica TCS SP8, Germany).

1.2. Hydroxyl radical experiments using flow cytometry

Flow cytometry was used to detect hydroxyl radical formation. Hydroxyphenyl-fluorescein (HPF) is an anthracene derivative of fluorescein which becomes fluorescent when it was activated by hydroxyl radical (Shi et al., 2021). The bacterial culture with 8 Log CFU/mL *P. fluorescens* was treated with or without OG under BL exposure for 20 min. Samples without irradiation were chosen to be controlled. After various treatments, fluorescent reporter dye 3'-(p-hydroxyphenyl) fluorescein (HPF, Invitrogen) was added into the solution to reach a final concentration of 10 μM, and the mixture was incubated at 37 ºC for 30 min. Then, samples were centrifuged at 10000×g for 5 min and washed twice in PBS to remove excess dye. The cell pellet was resuspended in PBS for the following measurement. For visualization of intracellular •OH in *P. fluorescence*, the fluorescent signal (λex/λem = 490/515 nm) was recorded by CytoFLEX flow cytometry (Beckman Coulter, USA). Calibrite beads (Becton Dickinson) were used for instrument calibration. Flow data were processed and analyzed with MATLAB (The MathWorks).

1.3. Investigation of the cell membrane damage

To evaluate the cell membrane damage induced by OG+BL treatment, the fluorescence probe

propidium iodide (PI) and scanning electron microscope (SEM) was performed (Shi et al., 2020; 2021). In brief, a sample containing 8 Log CFU/mL *P. fluorescens* and either 0 or 0.4 mM OG was exposed to BL for 20 min. Cells were then harvested from 1 mL volume of the incubated sample by centrifuging at 10000×g at room temperature for 5 min twice with an intermediate washing step using sterile DI water. The pellet was then re-suspended in 10 μM PI solution (1 mg/mL) following dark incubation at room temperature for 15 min. Subsequently, the incubated solution was washed with PBS and centrifuged for 2 min at 10,000×g. The pellet was resuspended in 500 mL PBS, and a 100 μL of each solution was transferred into a 96 well plate. The fluorescence spectrum was measured at excitation wavelengths of 495 with emission range from 500 to 800 nm with a microplate reader (Synergy H1 Multi-Mode Reader, BioTek, Winooski, VT, USA). Bacterial suspension with water kept in the dark was used as a control, and its fluorescence intensity reading was used as the reference to calculate the relative fluorescence unit (RFU) for other treatments using the following equation:

$$I_{corrected} = I_s - I_0$$

where I_s stands for the fluorescence emission intensity reading of the sample received treatments and I_o stands for the signal intensity of the control sample.

Scanning electron microscopy (SEM) was conducted to analyze the damage to the cell membrane caused by the OG+BL treatment. Briefly, the cultured samples containing 8 Log CFU/mL of *P. fluorescens* were treated with BL for 20 min. Controls consisted of bacterial suspension without OG in the dark and only exposure to OG. Following treatment, 1 mL bacterial suspension was centrifuged for 5 min at 6000 rpm and washed with PBS, then, the samples were resuspended with 2.5% glutaraldehyde for overnight at 4 ^{o}C. Finally, the samples were dehydrated sequentially in 25, 50, 75, 95% and 100% (v/v) aqueous solutions of ethanol following washed with PBS. Cells were placed on a SEM stub and coated with gold to observe the morphology with a Hitachi T-1000 scanning electron microscope (Hitachi High-Technologies Corporation, Tokyo, Japan) an acceleration voltage of 15 kV.

1.4. Sodium dodecyl sulfate-polyacrylamide gel electrophoresis (SDS-PAGE)

SDS-PAGE analysis was performed to determine the alternations of bacterial proteins before and after the treatment of OG and BL irradiation. OG-mediated PDI treated *P. fluorescens* (8 Log CFU/mL) was collected by centrifugation (10000×g, 4 ^{o}C) for 5 min, and then washed 3 times using PBS (0.1 M, pH 7.2). The proteins were obtained using kits (BestBio, Shanghai, China) and

then mixed with loading buffer at 100 ºC for 10 min. Subsequently, the Marker (Takaba, Dalian, China) and proteins were run through the 12% separating gel and 3% stacking gel at 100V for 90 min. The gel was stained using Coomassie brilliant blue (R-250) stain solution for 4 h. Afterward, the gel was destained with a common decoloring agent.

1.5. Genome integrity determination

The damage of DNA caused by OG+BL was investigated by the agarose gel electrophoresis. Briefly, the OG+BL treated *P. fluorescens* (~8 Log CFU/mL) was centrifugated at 6000×g for 5 min, and the bacterial DNA was extracted using a DNA extraction kit (Sangon, Shanghai). The samples were separated by 1% agarose. The parameters of the DNA electrophoresis instrument were set to a voltage of 100 V for 30 mins. The gel images of samples were observed and recorded on a ChemiDoc MP Imaging System (Bio-Rad, Hercules, CA, USA).

1.6. Confocal laser scanning microscopy (CLSM)

To observe the formation of the biofilm after various treatments, samples were captured by CLSM refer to Seo and Kang (2020) with some modifications. *P. fluorescence* was treated as described above, Then, bacteria were cultured in a Confocal Quartz Petri Dish at 30 °C for 60 h, after cultivation, planktonic cells were removed by gently washing the dishes with 0.9% sterile normal saline. For visual observation of the performed biofilms after different treatments, *P. fluorescence* was cultured in a Confocal Quartz Petri Dish using the method above, and then planktonic cells were removed by gently washing the dishes with PBS, after that, preformed biofilms were treated with different conditions. Treated biofilm was then stained using a LIVE/DEAD *Bac*light Bacterial Viability Kits (Molecular Probes, Invitrogen, USA) according to the manufacturer's instructions. The biofilm was washed with PBS and visualized using a CLSM. The 20×objective was used to monitor STYO 9 fluorescence excited at 488 nm and emitted at 493-580 nm, propidium iodide fluorescence excited at 552 nm and emitted at 566-719 nm.

1.7. Preparation of nanofibers (NFs)

The NFs were prepared using the method reported by us (Shi et al., 2020) with some modifications. Briefly, the solutions used for electrospinning were obtained by dissolving poly(lactic acid) (PLA) in hexafluoroisopropanol (HFIP) (9%, *w*/*v*, 0.9 g of PLA in 10 mL HFIP) at room temperature under

stirring for 3 h. The OG/*β*-cyclodextrin inclusion complexes (OG/*β*CD, 6% and 8%, *w*/*v*) were added to the solution with magnetically stirring for 12 h at room temperature to obtain the homogeneous solution for electrospinning. The prepared solution was put into a 10 mL polypropylene syringe fitted with a 23G (outer/inner diameter; 0.64 mm/0.33 mm) metallic needle. The solution flow rate was 0.9 mL h^{-1}. The loaded syringe was fixed horizontally with a syringe pump (Baoding longer, LSP03-1A) and the electrode of the high voltage power supply (Tianjin Dongwen, DWLP303-1ACDB) was connected to the metal needle tip. The working distance between the needle tip and the ground electrode was 10 cm. The electrospinning voltage was 18 kV. The electrospinning temperature and the relative humidities were 25 ºC and 45%, respectively. The collected fibers were vacuum dried for 24 h to remove solvent residue and their morphology was observed via SEM (Hitachi T-1000, Hitachi High-Technologies Corporation, Tokyo, Japan) (see Fig. S1) and the preservation of giant salamander (Fig. S4).

1.8. In situ antibacterial activity of OG/PLA NFs

To assess the synergistic effect of OG/PLA NFs and PDI on the preservation of Chinese giant salamander, the changes in the total viable count and flavor of samples during storage were studied. The salamander meat cubes (4 cm×4 cm×1 cm, 10 g) were cut under aseptic conditions, then inoculated by immersion in a bacterial suspension of *P. fluorescens* (3 Log CFU/mL) for 30 seconds and then all samples were dried at room temperature for 10 min and the treated salamander meats were singly sealed with OG/PLA NFs and followed immediately by BL exposure (Radiation intensity: 213 mW/cm^2) for 30 min at a distance of 1 cm. The bacteria were collected from the surface of meat using PBS (0.1 M, pH 7.2). The viable cell count was determined by placing them on LB agar plates after serial dilution. To further investigate the effect of OG/PLA NFs combined with PDI on the preservation of Chinese giant salamander, the changes in the total viable count and flavor of samples during the storage were studied. All samples were stored at 4 ºC for 15 days. The colonies were counted at intervals of 3 days. Meanwhile, to evaluate the quality of the giant salamander with different treatments during the storage, the electronic nose was applied to analyze the flavor on the salamander from batches control, control+BL, OG/PLA NFs and OG/PLA NFs+BL at 4 ºC for 15 days (for more details was given in SI-Section 1.2). Each group was analyzed three times in parallel.

152 *1.9. The electronic nose*

153 The flavor analysis using an electronic nose was also performed on salamander from batches
154 control, control+UV-A, OG/HPβCD NFs and OG/HPβCD NFs+UV-A at 4 ^{o}C for 15 days. Five
155 repetitions were performed for each group. The electronic nose (Figure S1) applied in the
156 experiment was also developed by us. It consists of a sampling system, a detector containing the
157 array of sensors, and pattern recognition for data recording. The sensor array is composed of
158 fourteen different metal oxide sensors. Each sensor has a certain degree of affinity toward specific
159 chemicals or volatile compounds. The sensors' response to changes in conductivity induced by the
160 adsorption of gas-phase molecules and on subsequent surface reactions. Before the measurement,
161 the system of the electronic nose was cleaned with zero-air which was indoor air-filtered by active
162 carbon. The main purpose of zero-air was to clean the circuit and to return the sensors to the
163 baselines. During the measurement of icefish, the headspace gas of a sample was pumped into the
164 sensor chamber at a constant rate of 0.6 L/min through a tube connected to a needle. The response
165 of each sensor was expressed as a ratio of conductance (G/G0, G and G0 are conductances of the
166 sensors' response to the sample gas and the zero-air, respectively). The measurement procedure was
167 controlled by a special program. The measurement time was 160 s, which was sufficient for each
168 sensor to reach a stable value. The cleaning time was set to 100 s. The data was stored after the
169 measurement was completed. The same sample was paralleled 5 times.
170
171

2. Results

Table S1. MIC and MBC of **GA** or **OG** against *P. fluoresens* and *S. aureus*.

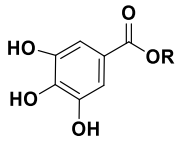		R	*P. fluoresens* (G^-)		*S. aureus* (G^+)		*c*Log *P*[a]
			MIC (mM)	MBC (mM)	MIC (mM)	MBC (mM)	
Gallic acid	**GA**	H	6.4	6.4	3.2	>6.4	0.4254
Octyl Gallate	**OG**	C_8H_{17}	0.1	3.2	0.05	0.1	4.6344

[a] Theoretical estimate using ChemBioDraw Ultra 13.0 program. Hydrophobicity of GA and OG from their partition coefficient (Log*P*) analysis. Log*P* is defined as the decadic logarithm of the particular ratio of the concentration of a compound between the two solvents (octanol phase and water phase).

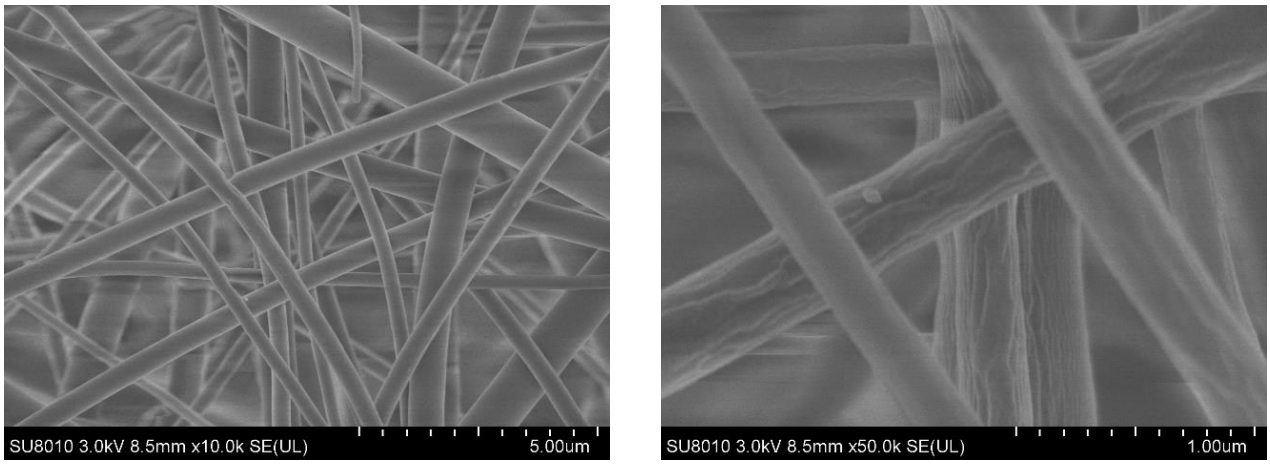

Fig. S1. SEM images PLA-OG/*β*CD nanofibers.

The morphological analysis of the composite electrospinning nanofibers containing OG was carried out using Hitachi T-1000 scanning electron microscope (Hitachi High-Technologies Corporation, Tokyo, Japan), with an acceleration voltage of 15 kV, as shown in Fig. S1. The composite nanofibers were set on a metallic stub and covered with gold under vacuum in an argon atmosphere.

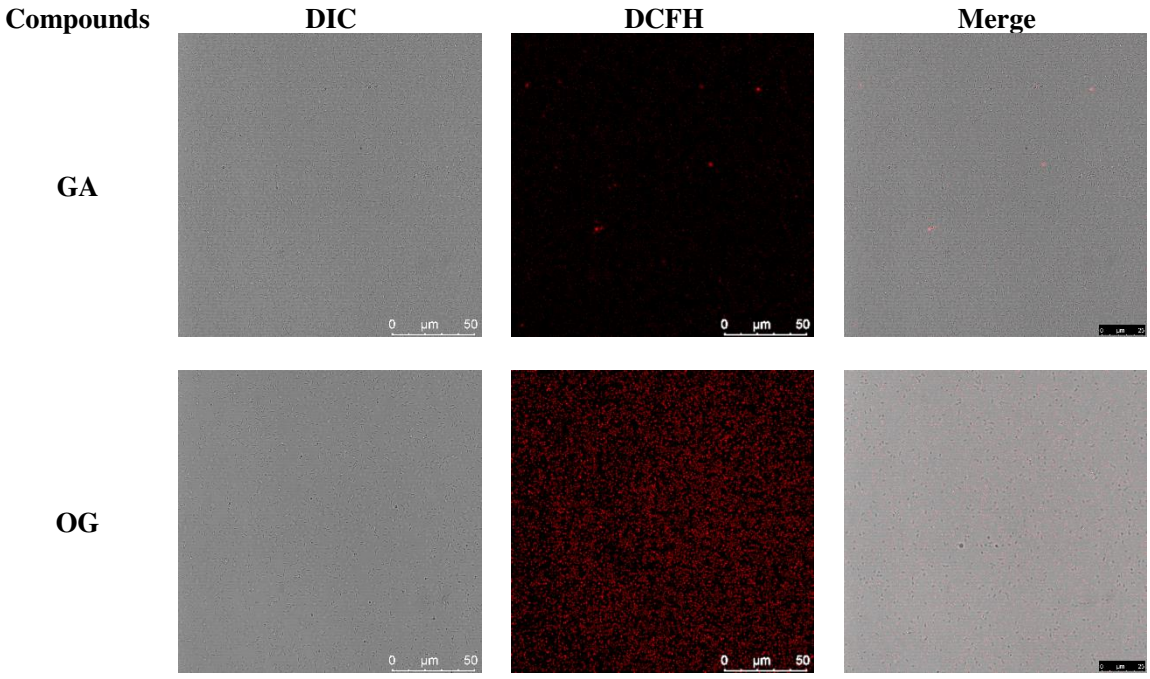

(B)

Fig. S2. Confocal laser scanning microscopy images of GA or OG in *P. fluorescens* stained with DPBA.

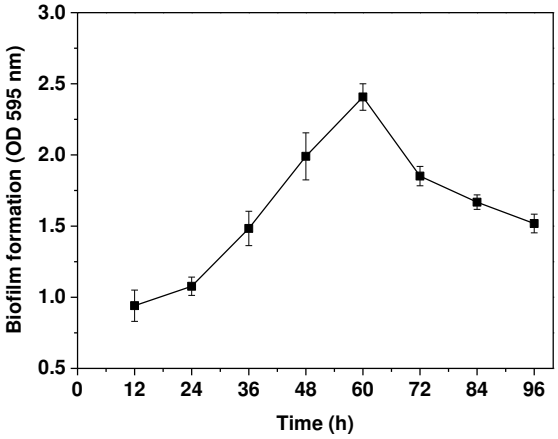

Fig. S3. Quantitative analysis of biofilm biomass.

205

206
207
208

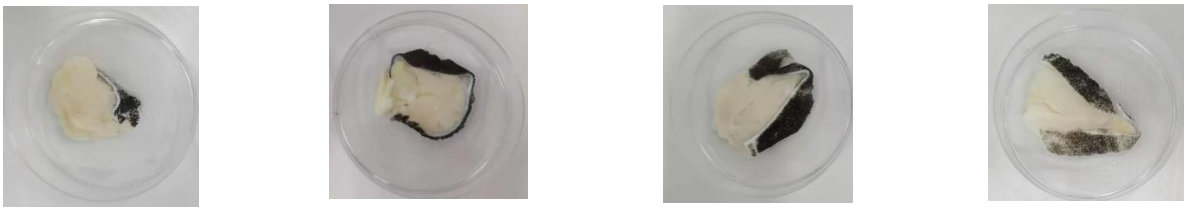

(a) (b) (c) (d)

Fig. S4. Physical appearance of Chinese giant salamander treated with (a) control ; (b) BL; (c) OG/PLA NFs; (d) OG/PLA NFs + BL (a-d: 4 ^{o}C, 15days)

209
210

211 **TOC GRAPHIC**

212

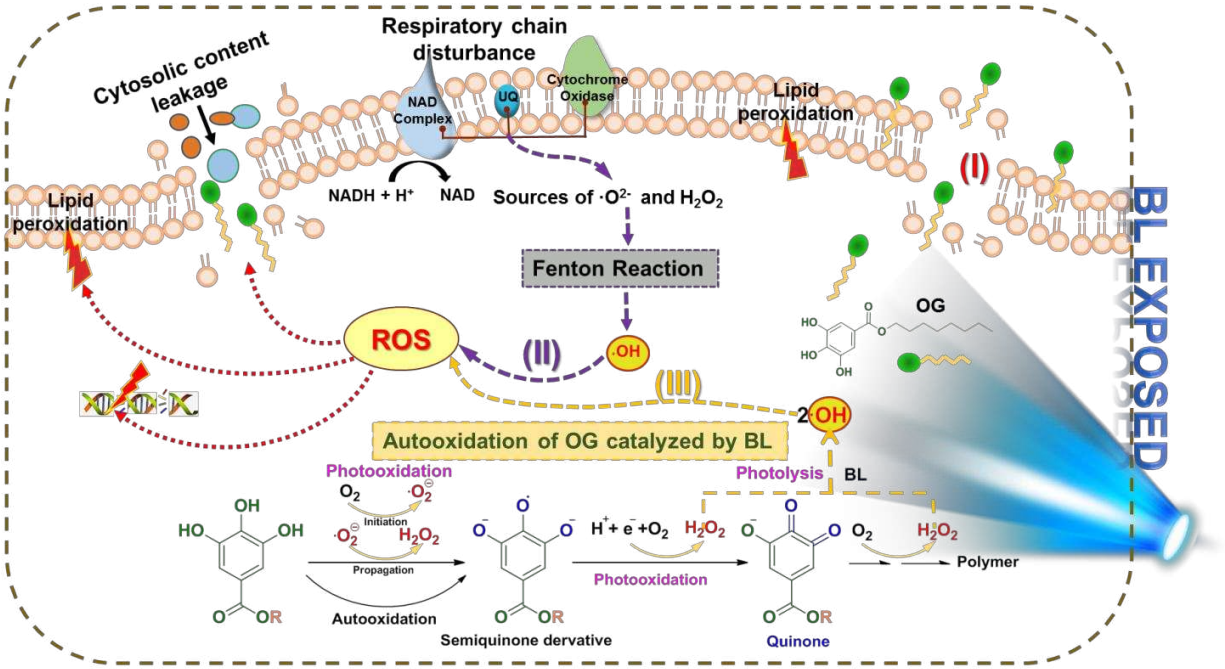

213

Declaration of interest statement

We declare that we have no financial and personal relationships with other people or organizations that can inappropriately influence our work, there is no professional or other personal interest of any nature or kind in any product, service and/or company that could be construed as influencing the position presented in, or the review of, the manuscript entitled.